Response to the Associate Editor

For both the main text and the Supplement:
The numeric concentration data and the percentage concentrations are given with too many significant figures. Three significant figures suffice when the first significant figure is a "1" and two significant suffice in the other cases.

Tables 1, 2, S1, S2, and S3 were modified according to the suggestion. We also changed the values in the text (Section 3.3) accordingly.

For the main text:
Page 1, line 29: Replace "proton-induced" by "particle-induced". Done.
Page 1, line 30: Replace "i.e. sample" by "i.e., sample". Done.
Page 1, line 33: Replace "e.g. a" by "e.g., a". Done.
Page 1, line 34: Replace "e.g. Annegarn" by "e.g., Annegarn". Done.
Page 1, line 36: Replace "XRF" by "The XRF". Done.
Page 2, line 11: Replace "e.g. resuspension" by "e.g., resuspension". Done.
Page 2, line 17: Replace "i.e. with" by "i.e., with". Done.
Page 2, line 19: Replace "by (Park et al., 2014)" by "by Park et al. (2014)". Done.
Page 3, line 1: Replace "13 Aug" by "13 August". Done.
Page 3, line 23: Replace "samples collection" by "sample collection". Done.
Page 4, line 8: Replace "is same" by "is the same". Done.
Page 4, line 16: Replace "for lightest" by "for the lightest". Done.
Page 5, line 22: Replace "TEOM data" by "the TEOM data". Done.
Page 5, line 25: Abbreviations and acronyms (here "DAQ") should be defined (written full-out) when first used. Done. We replaced “an erroneous DAQ value” with “software malfunction”
Page 5, line 29: Replace "e.g. according" by "e.g., according". Done.
Page 5, line 31: Replace "value where" by "value, which were". Done.
Page 5, line 39: Replace "1 Aug" by "1 August". Done.
Page 6, line 27: Replace "e.g. blank" by "e.g., blank". Done.
Page 7, line 11: Replace "to Gerboles" by "to those in Gerboles". Done.
Page 7, line 20: Replace "e.g. an" by "e.g., an". Done.
Page 7, line 24: Replace "i.e. of" by "i.e., of". Done.
Page 7, line 25: Replace "Hg were" by "Hg, which were". Not agreed.
Page 7, line 32: Replace "Jul and 1 Aug" by "July and 1 August". Done.
Page 7, line 37: Replace "of these two elements reflect" by "of Sb and Sn reflect". Done.
Page 8, line 21: Replace "2 Aug" by "2 August". Done.
Page 8, line 24: Replace "e.g. at" by "e.g., at". Done.
Page 8, line 33: Replace "1 Aug" by "1 August". Done.
Page 9, line 2: Insert a space between "period," and "the". Done.
Page 9, line 3: Replace "e.g." by "e.g.,". Done.
Page 9, line 7: Replace "e.g. elemental" by "e.g., elemental". Done.
Page 9, line 19: Replace "2 Aug" by "2 August". Done.
Page 9, line 24: Insert a space before "μg". Done.
Page 9, line 26: Replace "in brackets" by "in parentheses". Done.

Page 9, line 37: Abbreviations and acronyms (here "eBC") should be defined (written full-out) when first used. Done.
Page 10, line 2: Replace "e.g. Sr" by "e.g., Sr". Done.
Page 10, line 7: Replace "e.g. Hopke" by "e.g., Hopke". Done.
Page 10, line 25: Replace "inversion. . It" by "inversion. It". Done.
Page 11, line 14: Replace "comprised of approximately" by "comprised approximately". Done.
Page 11, line 19: Replace "Measured concentrations" by "The measured concentrations". Done.
Page 11, line 23: Replace "dependent on elements" by "depending on the element". Done.
Page 11, line 38: Replace "e.g. 2" by "e.g., 2". Done.
Page 12, line 5: Replace "Continuous" by "The continuous". Done.
Page 12, line 24: Replace "M.C.Minguillón" by "M.C. Minguillón". Done.
Pages 12-15, Reference list:
- abbreviated journal names should be used throughout; Checked.
- titles of journal articles should be in lower case and not in Title Case. Checked.
Page 15, lines 39-42: Yatkin et al. (2012) should come before Yatkin et al. (2016). Done.
Page 17, Figure 2: The text in the right ordinate does not come out properly. Figure exchanged.
Page 19, legend of Figure 4: Replace "elemnt" by "element". Done. Also removed hyphen in Xact-625.
Page 19, caption of Figure 4: Replace "Xact625" by "Xact 625". Done.
Page 20, ordinate of Figure 5: Replace "Xact625" by "Xact 625". Done.
Page 28, footnote 2) of Table 2: Replace "Gälli" by "Gälli Purghart". Done.
Page 28, footnote 7) of Table 2: "Alastuey et al. 2016" is not in the Reference list. Done.

For the Supplement:
Page 1, line 2: Replace "Table 2)" by "Table 1)". Done.
Page 1, line 16: Replace "47mm" by "47 mm". Done.
Page 1, line 22: Replace "Table S1" by "Table S2". Done.
Page 2, line 22: Replace "Table S2" by "Table S3". Done.
Page 3, line 4: Replace "Table S2" by "Table S3". Done.
Page 3, line 7: Replace "Tanner et al. 1974" by "Tanner et al., 1974". Done.

Elemental composition of ambient aerosols measured with high temporal resolution using an online XRF spectrometer

Markus Furger[1,*], María Cruz Minguillón[2], Varun Yadav[3], Jay G. Slowik[1], Christoph Hüglin[4], Roman Fröhlich[1], Krag Petterson[3], Urs Baltensperger[1], André S. H. Prévôt[1]

[1]Laboratory of Atmospheric Chemistry, Paul Scherrer Institute, 5232 Villigen PSI, Switzerland
[2]Institute of Environmental Assessment and Water Research (IDAEA), Consejo Superior de Investigaciones Científicas (CSIC), Jordi Girona 18-26, 08034 Barcelona, Spain
[3]Cooper Environmental Services (CES), 9403 SW Nimbus Avenue, Beaverton, OR 97008, USA
[4] Laboratory for Air Pollution / Environmental Technology, Empa, Überlandstrasse 129, 8600 Dübendorf, Switzerland

* *Correspondence to*: Markus Furger (markus.furger@psi.ch)

Abstract. An Xact 625 ambient metals monitor was tested during a three-week field campaign at the rural, traffic-influenced site Härkingen in Switzerland during summer of 2015. The field campaign encompassed the Swiss National Day fireworks event, providing increased concentrations and unique chemical signatures compared to non-fireworks (or background) periods. The objective was to evaluate the data quality by intercomparison with other independent measurements, and test its applicability for aerosol source quantification. The Xact was configured to measure 24 elements in PM_{10} with 1-h time resolution. Data quality was evaluated for 10 24-h averages of Xact data by intercomparison with 24-h PM_{10} filter data analysed with ICP-OES for major elements, ICP-MS for trace elements, and gold amalgamation atomic absorption spectrometry for Hg. Ten elements (S, K, Ca, Ti, Mn, Fe, Cu, Zn, Ba, Pb) showed an excellent correlation between the compared methods, with r^2 values ≥ 0.95. However, the slopes of the regressions between Xact 625 and ICP data varied from 0.97 to 1.8 (average 1.28) and thus indicated generally higher Xact elemental concentrations than ICP for these elements. Possible reasons for these differences are discussed, but further investigations are needed. For the remaining elements no conclusions could be drawn about their quantification for various reasons, mainly detection limit issues. An indirect intercomparison of hourly values was performed for the fireworks peak, which brought good agreement of total masses when the Xact data was corrected with the regressions from the 24-h value intercomparison. The results demonstrate that multi-metal characterization at high-time resolution capability of Xact is a valuable and practical tool for ambient monitoring.

1 Introduction

The quantification of trace elements in airborne particulate matter (PM) can be achieved with various techniques, such as inductively-coupled plasma mass spectrometry (ICP-MS), inductively-coupled plasma optical emission spectrometry (ICP-OES), X-ray fluorescence spectrometry (XRF), and ~~proton~~particle-induced X-ray emission spectrometry (PIXE). These methods require a two-step procedure, i.e., sample collection in the field followed by laboratory analysis. Ambient pollutants are conventionally collected on filter substrate for large time duration such as 8-h or 24-h sampling time to ensure that sufficient elemental mass is available for analytical analysis (ICP). For high time resolution, impactors are used where the sample is collected on a foil (e.g., a rotating drum impactor, Lundgren, 1967), or on a combination of an impactor plate and a filter, such as in a streaker sampler (e.g., Annegarn et al., 1992). These samples are then exposed to X-rays or a particle beam without further treatment, which provide quantitative data with low detection limits. In contrast to the non-destructive XRF method, sample preparation for ICP analysis is very laborious, and the samples are destroyed during this process. The XRF method has been successfully applied to aerosol characterization in the last decades. Measurement of low sample mass typically requires a high sensitivity (or a low mimimum detection limit, MDL) and hence access to a synchrotron or accelerator facilities (Bukowiecki et al., 2005; Bukowiecki et al., 2008; Calzolai et al., 2010; Calzolai et al., 2015; Lucarelli et al., 2011; Richard et al., 2010; Visser et al., 2015b; Yatkin et al., 2016), which is notoriously difficult due to the demand

for analysis time at such facilities. Access restrictions limit the number of collected samples to be analysed, and hence field campaigns are predominantly episodic. Technical advances in X-ray sources and detectors have recently resulted in the development of commercial systems capable of sampling and analysing ambient PM samples in sub-hourly or hourly resolution in quasi real time. Instruments of this type can be used for continuous (months, years) monitoring at a site, but their cost may restrict the simultaneous deployment of a larger number of devices for different size fractions or at different sites. The benefit of long-term, quasi real time data access, favourable, e.g., for air quality monitoring, contrasts with the possibilities of relatively low cost, multi-site and multi-size samplers used so far in episodic field studies.

Sampling with high time resolution generates large quantities of data capable of capturing source emission patterns occurring at shorter time duration. For source apportionment of PM components like elements, a high time resolution of the order of 1 hour or less is advantageous, as temporally variable environmental factors such as wind direction and speed or insolation may affect transport and source processes, e.g., resuspension (Annegarn et al., 1992; D'Alessandro et al., 2003; Sánchez-Rodas et al., 2007; Sarmiento et al., 2007; Visser et al., 2015b; Yadav and Turner, 2014). One such instrument, Cooper Environmental's Xact® 625 Ambient Metals Monitor, performs in-situ automated measurements of ambient PM_{10} or $PM_{2.5}$ elemental concentrations for a user-defined set of 24 or more elements with a user-selected sampling time resolution of 15 to 240 minutes. The instrument is transportable and can be deployed in field campaigns where a suitable shelter with electric power and an appropriate sampling line connecting the outdoor with the indoor is available. Remote access to the data is possible during operation, which allows for a continuous, quasi real time (i.e., with a delay of one sampling interval) monitoring of the operation status and the ambient metal content. An in-depth evaluation of the forerunner instrument Xact 620 was previously published by (Park et al., (2014).

An Xact 625 monitor was deployed for a month to test the handling and data production of the instrument. A small field campaign was organized at a monitoring station of the Swiss Air Pollution Monitoring Network (NABEL), where quality-controlled air pollution measurements are performed continuously. The NABEL network provided the reference for previous data intercomparisons (Hueglin et al., 2005; Lanz et al., 2010), as well as for the intercomparisons of this study. Comparisons between SR-XRF and filter samples analysed with ICP-OES and ICP-MS have been performed previously (Richard et al., 2010). Comparisons of XRF on samples collected on different substrates were performed, e.g., by Yatkin et al. (2012). A recent interlaboratory comparison of PM_{10} filter analysis methods is presented in Yatkin et al. (2016), where XRF/PIXE and ICP methods were compared for several metrics. Some of these metrics are also applied in this study.

The goals of this article are 1) to characterize the measurements of the test period in Härkingen and compare them with previous studies in Switzerland and elsewhere; 2) to examine the achieved data quality for the selected elements with respect to their minimum detection limits; 3) to quantify the measurement quality based on intercomparisons between the Xact and NABEL PM_{10} data (1-h TEOM data and 24-h filter samples) for Härkingen; 4) to evaluate the applicability of the instrument at high time resolution in typical summer conditions and concentration ranges at a traffic-influenced rural site in Switzerland; and 5) to gauge the advantages of high time resolution sampling for a preliminary investigation of sources based on enhancement ratios and diurnal variability of elements. A pollution episode captured during the campaign resulted in high ambient concentrations, widening the range of studied concentrations. The selected elements represented a typical mix of elements at the selected site. In addition, a few elements notoriously difficult to measure in Switzerland due to their generally low ambient concentration were included, namely Ni, As, Pt, and Hg.

2 Experimental setup

2.1 Site characteristics

The field campaign was performed at the permanent station Härkingen (47.311877° N, 7.820453° E) of the Swiss Air Pollution Monitoring Network (NABEL, http://www.bafu.admin.ch/luft/00612/00625/index.html?lang=en) from 23 July

until 13 August 2015. This station is located next to the A1 freeway, the main traffic route between eastern and western Switzerland. About 1 km to the west the A2 freeway branches off towards the north. The local terrain is level and the traffic flows freely even during rush hours, limiting incidences of excessive braking or forced acceleration. There are villages to the south and east of the site, and agricultural land immediately to the west and north. Other local activities include industrial buildings approximately 500 m to the northwest (logistics businesses), and a metal processing company to the southeast across the freeway. The site is well documented with respect to gas phase traffic emissions, PM number concentrations and particulate elemental carbon (EC, Hueglin et al., 2006), but an in-depth local source apportionment has not been realised so far except for organic aerosols measured in May 2005 (Lanz et al., 2010).

The first week of the campaign was characterized by moderate summer temperatures (maximum temperature <25 °C, except 23 July) with some occasional rain cleansing the atmosphere. The remaining two weeks were part of a summer heat wave, with temperatures reaching 36.4 °C at the maximum, and values above 30 °C on 7 days of this period. Only one precipitation event occurred during the hot period. The Swiss National Day (1 August) fell on a Saturday, and the weekend weather promoted outdoor barbeques and fireworks. The bulk of the fireworks were burnt on 1 August after 2200 LT (local time = UTC + 2 h), but some individual fireworks were also burnt on 31 July, and 2 and 3 August.

For this study, the Xact 625 monitor and a Q-ACSM (quadrupole aerosol chemical speciation monitor, Aerodyne Inc.) were installed in an air-conditioned trailer parked next to the NABEL station. This trailer was placed to the north of the freeway at ~23 m away from the centre of the freeway. This placed the trailer on the orthogonal transect between the freeway and NABEL shelter, which is located ~27 m from the centre of the freeway. The trailer's instruments were connected to the NABEL station's power grid and Ethernet.

2.2 NABEL instrumentation

The NABEL station is equipped with a broad range of air quality instrumentation and standard meteorological sensors. The relevant instruments for this field test were the Digitel DA-80H HiVol sampler with a DPM 10/30/00 inlet for 24-h PM_{10} samples collection, and a TEOM FDMS 8500 (Tapered Element Oscillating Microbalance, Filter Dynamics Measurement System, Thermo Scientific) for continuous (10-min) PM_{10} mass concentration measurements. The time constant used for noise reduction in the TEOM and the averaging procedure caused a significant time delay in peak concentrations. For 1-h values, the random error of a TEOM as derived from parallel operation of two identical instruments is about 2 µg m^{-3}. Standard meteorological measurements such as temperature, wind speed and direction, and precipitation records are also monitored at this station. Furthermore, the station also provided hourly traffic counts for the freeway in the form of total number of vehicles, number of heavy duty vehicles (HDV), and number of light duty vehicles (LDV).

2.3 Xact 625

The Xact 625 ambient metals monitor (Cooper Environmental Services (CES), Beaverton, OR, USA) is a sampling and analysing X-ray fluorescence spectrometer designed for online, semi-continuous measurements of elements in aerosols. In this study, ambient air was sampled with a flow rate of 16.7 actual lpm through a PM_{10} flow separator (Tisch Environmental, TE-PM10-D) and the PM collected onto a Teflon filter tape. The flow is maintained to within about 1 %. After each sampling interval the filter tape is moved into the analysis area of the spectrometer, where it is illuminated with an X-ray tube with three excitation conditions, and the excited X-ray fluorescence is measured with a silicon drift detector (SDD). During this XRF analysis, the next sample is collected on a clean spot of the filter tape. This cycle is repeated during each sampling interval, which was configured to be 60 minutes for this study. While this approach is non-destructive, the samples collected are typically not amenable to offline analysis post-sampling due to potential for cross-contamination from sampled filter tape wound upon itself onto the filter wheel. After each analysis interval, raw and calibrated (for the actual volume in units of ng m^{-3}) concentration data was stored on the hard disk of the control unit. Daily advanced quality assurance checks

(QA energy calibration test, QA upscale test) were performed during 30 min after midnight to monitor shifts in the calibration. Thus, the sampling interval following midnight was limited to 30 min only.

The instrument was configured to quantify 24 elements (Si, S, Cl, K, Ca, Ti, V, Cr, Mn, Fe, Co, Ni, Cu, Zn, As, Se, Cd, Sn, Sb, Ba, Pt, Hg, Pb, Bi, plus Pd for QA). Each of these elements was calibrated individually with a reference sample. Minimum detection limits (MDL) for 1-h sampling for each element are listed in Table 1. CES calculates MDLs using the sensitivity of the element and the counts in the region of interest of a blank unsampled section of tape, from where one sigma interference free detection limits are reported. XRF based MDLs are inversely proportional to the square root of the X-ray analysis time (Currie, 1977), which in the case of Xact is the same as the sampling duration. Hence, Xact MDLs are lower for longer sampling durations. Interference free MDLs, while true are idealized lower limits of detection of one single element. As with most analytical methods, matrix effects in ambient samples from interferences between different elements and analyte concentrations could potentially result in MDLs of ambient samples to be higher and vary across samples, which makes them difficult to generalize and report. It is therefore often preferred to report measurement uncertainties to characterize a measurement. An uncertainty of 5 % or less due to fitting errors and uncertainties in the standards has been derived from laboratory experiments with NIST standards (benchtop XRF, filter analyses). Uncertainties are expected to be higher for concentrations close to the MDL; for elements with potential for line interferences in multi-element samples; and, from self absorption effects for the lightest elements (Si, S, Cl, K, Ca). Line interference is well-known for element couples like Fe-Co, Pb-As, Ba-Ti and makes detection of one element difficult if the other is abundant in the sample. The linear least squares reference deconvolution algorithm implemented in the Xact fits the measured sample spectrum with the library of pure element reference spectra to resolve concentrations of each calibrated element. The Xact reports purely elemental mass concentrations, which are the focus of discussion and unless otherwise noted.

2.4 Q-ACSM

A Q-ACSM (Aerodyne Inc., Billerica, MA, USA) was operated in the trailer housing the Xact 625 during the campaign. The Q-ACSM determines quantitative mass spectra of non-refractory particles up to mass to charge ratios (*m/z*) of 150 (Crenn et al., 2015; Ng et al., 2011). Ion fragments were attributed mainly to organic aerosols, nitrate, sulphate, ammonium, and chloride, which comprise the reported data used in this study. The collection efficiency (CE) was determined for each spectrum according to Middlebrook et al. (2012), and its distribution peaked at the mode of 0.62 (±0.11). 293 out of 1055 CE values of the full ACSM dataset were equal to 0.45. The Q-ACSM collected sub-micron (PM_1) particles and chemically analysed them in 30-min intervals, which were aggregated to 1-h averages for comparison with the Xact 625 data. All concentrations used in this study were CE corrected.

2.5 24-h PM_{10} filter samples

The 24-h PM_{10} samples collected by the HiVol sampler on quartz filters were weighed at Empa laboratory in Dübendorf, Switzerland to determine the gravimetric daily PM_{10} concentrations. These values were then used to correct the TEOM PM_{10} concentrations on a daily basis. Therefore the 24-h TEOM values correspond to 24-h gravimetric PM_{10}. Ten 24-h PM_{10} samples were analysed for their elemental composition at IDAEA-CSIC laboratory in Barcelona. A quarter of each filter was acid digested using a mix of HF:HNO_3 (2.5:1.25 mL), the solution was kept in a Teflon reactor at 90°C for at least 6 h, and after cooling 2.5 mL of $HClO_4$ were added. The acid solution was brought to evaporation and the dry residual was re-dissolved with HNO_3 and diluted with milli-Q water for subsequent ICP-OES and ICP-MS analysis. This method has been validated and used in many studies, and is discussed in detail elsewhere (Minguillón et al., 2012; Querol et al., 2001; Querol et al., 2008). A total of 41 elements from Li to U were analysed: the major elements Na, Mg, Al, P, S, K, Ca, Ti, and Fe with ICP-OES; the trace elements with ICP-MS. Si, Cl, and Pt were not analysed on the filters. Analyses of the reference material NIST 1633b (constituent elements in coal fly ash) using the same methodology as that for the samples yielded satisfactory

results, with approximately 100% recoveries for the elements under study. Tests of the used methodology with respect to other ICP sample preparation and analysis methods, and applications of the methodology to NIST standards indicated the reliability of the method, exerting a maximum scatter of 10 % for any of the elements, with most uncertainty values clearly below this limit. Relative uncertainties (precision) of the ICP measurements are less than 5 % for the elements with concentrations well above their respective detection limits, whereas the overall uncertainty reflecting the entire sampling procedure, the digestion and the ICP analysis is on the order of 25 %. Minimum detection limits for ICP were determined according to Escrig et al. (2009), and the values for the elements relevant for our intercomparison are listed in Table 1. Hg was analysed with a Hg gold amalgamation atomic absorption analyser (AMA-254, LECO instruments, Botasini et al., 2013; Diez et al., 2007). The three methods are referred to as the offline or ICP methods (ICP-OES, ICP-MS), and the Hg gold amalgamation atomic absorption spectrometry is abbreviated with AuAAA in this paper.

Three of the 10 filters were also analysed with a benchtop XRF system by CES, and with ICP-MS by an independent lab (Eastern Research Group, ERG, Research Triangle Park, NC, USA) to investigate inter-laboratory scatter. ERG used a different digestion method than IDAEA-CSIC. In addition, three filters were prepared with a reference aerosol of known concentration for Fe, Cu, Zn, Sr and Pb, which then were analysed by CES, IDAEA-CSIC, and ERG, again to gain insight into the inter-laboratory scatter. Details on these data and the methods are given in the supplement of this article.

2.6 Data coverage and synchronization

The Xact 625 measurements started on 23 July 2015 1200 LT, and ended on 13 August 2015 0600 LT. The sampling interval was set to 1 h. Two interruptions occurred during the sampling period: one due to an Xact 625 computer problem (33 h), the other one due to a delayed filter tape change (10 h). The Xact dataset consists of 456 valid 1-hour samples out of 499 possible samples, attaining a coverage of 91.4 %. The NABEL data were tailored to coincide with the Xact data. The 10-min TEOM PM_{10} values were aggregated to 1-h values to synchronize them with hourly Xact 625 measurements. Additionally, the TEOM data were also adjusted to the gravimetrically determined PM_{10} masses from the HiVol filters to provide an independent reference for intercomparisons. The data used here contained some gaps which were only partly synchronous for the selected parameters. Wind speed and direction missed 12 data points (2.4 %), precipitation 26 (5.2~~1~~ %), and PM_{10} 53 (10.6 %) at hourly time resolution. The ACSM data contained a gap of 14.5 h due to ~~an erroneous DAQ value~~software malfunction, which caused the data to be very noisy for that short period. These values were rejected from the analyses, and only the remaining 972 data points were averaged to 465 1-h values, which then were resampled to the 456 Xact data points.

For the comparisons of the different instruments and sampling intervals, all data were resampled to the corresponding times of the Xact 625, according to the sub-classifications of the data set (e.g., according to wind sectors). For the intercomparisons with the 10 filter samples, the hourly Xact data of the corresponding days were averaged to the 24 h of the filter samples. During each 24-h period, Xact generated 23 1-h values and 1 30-min value, which were aggregated to 24-h daily averages. This procedure implicitly assumes that the half-hour sample of the first sampling hour is representative for the whole hour. Tests with a 23.5-h weighted average yielded differences of less than 3 % between the two calculation methods. Comparisons of hourly Xact data were only possible for S with the ACSM data (in the form of PM_1 sulphate, assuming that all S occurs in PM_1), and between the total Xact element mass and PM_{10} of the NABEL TEOM instrument, see Sections 3.2 and 3.3.

3 Results and discussion

3.1 Data validity derived from general statistics and minimum detection limits

The complete Xact dataset is visualized in Figure 1, and general statistics are given in Table S1. The salient feature of the concentration time series is the huge peak late on 1 August, caused by the National Day's fireworks episode. Further peaks before and after that day warranted dividing the full data set into a fireworks period and a non-fireworks period. The fireworks period started on 31 July 2015 2200 LT and lasted until 4 August 2015 1100 LT, as will be discussed in more detail in Sect. 3.3. The remaining non-fireworks period is representative for the typical background concentrations at Härkingen, and can be compared to literature values.

MDLs for the Xact 625 and for ICP-OES/MS and the Hg AuAAA method are listed in Table 1. Note that MDLs of elements measured by Xact 625 are based on 1-hr sampling time while MDLs of filter based elemental concentrations are based on 24-hr. Generally, values below 3*MDL are expected to have much higher uncertainty. Hence, elements with more than 80 % of the data below 3*MDL were rejected from further examination. Xact 625 MDLs have not been determined by the manufacturer for Si, S, and Cl, because self-absorption effects for elements lighter than Ca become more important with decreasing atomic number (Formenti et al., 2010). However, these three elements are abundant, and we assume that they are well above their Xact detection limit. For these elements, an ICP MDL is only given for S, because Si cannot be determined in the filter samples, as it is a main constituent of the quartz filters and is also digested during sample preparation, and Cl cannot be determined by ICP. The table indicates the amount of data points >MDL in percent for the different analysis methods. The elements K, Ca, Ti, Mn, Fe, Cu, Zn, Sn, Sb, Ba, and Pb have most values above the MDL, and their measurement should thus be reliable. Seven Xact elements have >50 % of their data points below MDL and more than 90 % below 3*MDL: V, Co, As, Se, Cd, Pt, and Bi. Cr and Cd show the same behaviour for ICP. Ni revealed variable blank concentrations in the filters and could therefore not be reliably measured with ICP. Hg is also mostly below MDL in the AuAAA measurement, and Pt was not measured with ICP at all. In summary, 11 elements (K, Ca, Ti, Mn, Fe, Cu, Zn, Sn, Sb, Ba, Pb) are above their MDLs for both the XRF and the offline methods, 7 elements (V, Co, As, Se, Cd, Pt, Bi) are below MDL for the XRF, and 3 elements (Cr, Cd, Hg) are below MDL for the offline methods (of which only Cd is below MDL for both XRF and ICP).

The comparisons between online Xact 625 and offline 24-h PM_{10} elemental concentrations for 21 elements are shown in Fig. 2, Fig. 3, and Table 1. Only the 21 elements analysed by both methods are compared by dividing them into two groups based on data characteristics.

Group A shows excellent correlations between the two measurement methods (r^2 values >0.95) and intercepts <40% of mean concentration, and consists of the elements *S, K, Ca,* Ti, *Fe*, Mn, Cu, Zn, Ba, and Pb (elements in *italics* were analysed with ICP-OES; the others by ICP-MS). The regression intercepts were not forced to be zero to enable examination of potential differences in the measurement accuracy of each of the compared methods, e.g., blank subtraction. The slopes are more relevant and indicate biases between the methods. Orthogonal least squares regressions metrics were calculated which incorporates measurement errors in both quantities being compared. The slopes differed by less than 3.5 % between the two regression methods for the Group A elements. Ba and Pb achieved an almost perfect match with slopes around 1 and negligible intercepts. The other extreme is Zn with a slope of 1.8. Ti is another peculiar case with a slope of 1.13 and the largest intercept/average concentration ratio of 0.37. On average, the Xact 625 yielded approximately 28% higher elemental concentrations than ICP for the Group A elements.

The high linearity and little scatter in the regressions testify for the precision of both the Xact and the ICP methods, but the differences in the slopes (range 0.97 to 1.8) for different elements require further investigation. No systematic deviations based on elemental molecular weight or X-ray excitation conditions were observed in these slopes. The deviations of the slopes from unity may be partially attributed to the different inlets for the Xact and the HiVol samplers (Panteliadis et al.,

2012), which may produce a difference in collected mass on the order of 10 %. The inlets were not explicitly tested for their cut-off characteristics in this study. A slightly different cut-off value for the particle size may lead to differences in the collected mass, especially for the largest and heaviest particles in PM_{10}, and hence to an underestimation or overestimation of the total mass collected with a particular inlet. This may be of special relevance in a near-road setting with lots of re-suspended dust (ACES, 2012). Potential line interference between Ti and Ba can be excluded, because the element couple reveals two different regressions for fireworks and non-fireworks cases, as well as distinct diurnal variations in the non-fireworks cases.

The results of additional investigations of a few selected filters by independent labs and analytical methods for understanding these differences are discussed in the supplementary material. Examination of reference samples indicated a high precision in XRF measurements despite consistently underestimated absolute concentration (underestimated by 6 to 14% depending on the element). In contrast, ICP measurements indicated greater variability (range of 30% underestimation to 60% overestimation, depending on the element) and hence higher uncertainty in estimated ambient concentrations. Examination of three filter samples collected during the campaign by an offline XRF instrument (by CES) and by ICP at an external laboratory (ERG) indicated a variability of about 30% for most elements, and an almost perfect match (-0~~,~~.1 %) between ICP labs for the average concentrations when Ca and Se are excluded, and deviations of less than 5 % between benchtop XRF and ICP (Table S2). These results are comparable to those in Gerboles et al. (2011). Comparisons between the Xact and benchtop XRF in previous tests by the manufacturer with better control of the sampler inlet conditions almost always were within 5 % of each other. The relative mean difference of 28 % between Xact and filter data (analysed with ICP) for samples collected during the field campaign appears to be systematic. Such differences may result from a difference in location of the Xact and filter sampling inlets (~5 m) and their relative distance from the freeway. Ultrafine particle number concentrations from dust resuspension due to vehicle traffic are known to decrease with increasing distance from the road, with the sharpest decline observed within the first 50 m (Hagler et al., 2009). Crustal elements, which dominate in the PM_{10} size fraction, are expected to settle faster due to larger aerosol size. Hence the difference in Xact and ICP reported PM_{10} elemental concentrations may be indicative of a gradient in PM occurring for some elements in close proximity to roadways. To quantify such near-source PM gradient, a field campaign with a different design would be needed, e.g., an array of samplers along a line perpendicular to the freeway. However, since the difference is also observed for S, which is typically found in the fine mode, does not have a major traffic related source apart from coarse re-suspended dust, and is not expected to suffer from incomplete digestion we assign part of the differences also to calibration issues with Xact.

Group B, the remainder, consists of the elements V, Cr, Co, As, Se, Cd, and Bi, i.e., of those elements that are close to or below their Xact MDL, plus Ni, Cd, Sn, Sb and Hg. Ni, Cd and Hg were below MDL for the offline methods (Cd for Xact and offline methods). Although an intercomparison of these elements may not be justified, we observed some features in the regressions of the Group B elements in Fig. 2 that are worth commenting. Cr is below the ICP-MS MDL for 60 % and below 3*MDL for all filter values, but 75 % are above the Xact MDL. The ICP measurement is below MDL because of the high and variable blank concentrations, which make a meaningful blank subtraction difficult, and which increases the Cr MDL in these samples. Although the slope of Cr is 1.23 and thus comparable to the other Group A slopes, a comparison with ICP values is statistically not robust. However, Cr seems to be quantifiable with the Xact. The regression plot of Bi shows two extreme values on 31 July and 1 August corresponding to the fireworks days. These two points are above MDL for both methods and suggest good quantitative agreement between XRF and ICP for these two high-concentration cases. Sb shows a moderate correlation (r^2 = 0.47), and a large intercept. Sn behaves similarly as Sb, with an r^2 value of 0.15. The large intercepts hint toward a problem in processing the Xact blanks. In addition, when Ca is abundant, as in our case in Härkingen, the Sb Lα line interferes with the Ca Kα line, producing low signal-to-noise ratios for Sb, and similarly for the pair K – Sn. Hence, the reported Xact concentrations of ~~these two elements~~Sn and Sb reflect mainly spectral noise. 60 % of

the filter Hg data were below MDL and thus cannot be well compared with the Xact Hg data. Inspection of the Xact raw Hg spectra showed a possible interference from Br causing the fitting routine to attribute some Br mass to non-existent Hg peaks in the spectra. Br was not calibrated in the fitting routine. Thus the Hg concentrations reported by the Xact seem to be due to this interference and are not realistic, even though 86 % of the measured values are above the Xact MDL. Values < 1.5 ng m^{-3} are in the same order of magnitude as the fortnight values of Chiaradia and Cupelin (2000) for the city of Geneva (Table 2). The element couples of Fe-Co and Pb-As do not show correlations within the couples, because most of their data points are below their respective MDLs, and no conclusion about the deconvolution of interfering lines can be drawn for these elements. Comparing the Xact values with the NABEL annual mean values (Table 2) shows differences smaller than 40 % for Cu, Pb, and Ni, while the differences are much larger for As and Cd. The latter two elements are below their respective MDL (Fig. 2). To summarize, the Group B elements show issues with the minimum detection limits of at least one of the analysis methods, which restricts thorough interpretation. Individual data points above MDL reveal nevertheless a usable quantification by the Xact in these particular cases. Determination of Sb, Sn and Hg by Xact are potentially impacted by XRF line interferences and warrant further improvements for better quantification by Xact.

The Group C elements Si, Cl, and Pt were not measured on the filters. An Xact MDL for S has not yet been determined. Data quality of S measurements was inferred by comparing its Xact concentrations with the concentrations of another element originating from the same source, or belonging to the same chemical compound. Xact reported S (with unknown MDL) and K (with known MDL) concentrations were highly correlated (r^2 = 0.99) during the fireworks period, with a slope of 2.30 ± 0.05, which agrees with the stoichiometric relation between K and S when forming K_2SO_4. For the non-fireworks periods the correlation was weak (r^2 = 0.16), which hints towards a completely different, more random relationship between the two elements, as expected. Hence, high concentration K reported by the Xact provided reliable S during the fireworks episode, despite the lack of an established MDL for S. Xact Pt measurements were always below MDL, and no conclusion about the Pt accuracy can be drawn.

3.2 Comparisons with other data

Figure 1 shows that roughly 95% of the total analysed elemental mass by Xact is comprised of 6 elements: Si, S, Cl, K, Ca, and Fe. These major elements all show average concentrations >100 ng m^{-3}. Si, S, Ca, and Fe are observed throughout the study, although with high variability. Cl and K are abundant only episodically: Cl is strongly tied to westerly winds during the last week of July, and is practically absent after 2 August. K is prominent during the fireworks period. Ti, Cu, and Zn show daily average concentrations between 11 and 34 ng m^{-3}. The other analysed elements were found in daily average concentrations <10 ng m^{-3}. The concentrations are of the same order of magnitude as those recently measured at other places in Switzerland, e.g., at an urban background site in Zurich (Minguillón et al., 2012; Richard et al., 2011, Table 2), but are generally lower than the measurements in older studies (Chiaradia and Cupelin, 2000; Gälli Purghart et al., 1990; Röösli et al., 2001, Table 2). The decreasing trends in PM and trace element concentrations have been documented in numerous NABEL reports on the air quality in Switzerland (e.g., BAFU and Empa, 2015; Gianini et al., 2012). These trends make it preferable to use modern studies for comparisons. Furthermore, the episodic nature of the 2015 campaign also demands for some generosity when comparing the measured values with annual or seasonal mean values.

A time series of the Xact 625 total element concentrations together with the NABEL TEOM PM_{10} data and the total ACSM non-refractory (NR)-PM_1 concentrations with 1-h resolution is presented in Figure 4. The total ACSM NR-PM_1 concentration is the sum of sulphates, nitrates, ammonia, chlorides and organic aerosols. Total PM_{10} shows a generally increasing trend over the whole campaign, with a strong peak superposed on 1 August 2015, whose increase coincides with the peak in the Xact data, whereas the maximum is delayed by one hour relative to the Xact data. The peak is due to the fireworks burnt on that evening. On average the Xact 625 elements make up about 20 % of the total PM_{10} mass (regression

slope 0.2, r^2 = 0.63). A complete mass closure cannot be achieved, because the NABEL station only reports the total gravimetric PM_{10} mass and $PM_{2.5}$ elemental carbon (EC) concentrations with diurnal or better time resolution.

Xact's measurement accuracy for S was tested by comparison with ACSM sulphate measurements (Figure 5) performed at 1-h resolution. The S concentrations of Xact 625 were multiplied with a factor of 3, assuming that all S occurred in the form of SO_4^{2-}. The slope of the regression line for the non-fireworks case is 1.34, with r^2 = 0.85, in line with the Group A elements, and in agreement with the comparison of S from Xact and from ICP, hence the slope between ACSM SO_4 and ICP SO_4 would be ~1. The high linear correlation suggests a high precision of the Xact 625 data, but does not allow a definitive answer on the accuracy because of expected self-absorption effects, which would increase the slope further if corrected. During the fireworks period, the scatter is large, and the correlation coefficient is only 0.1. We hypothesize that fireworks produce larger and non-refractory particles (e.g., K_2SO_4) not measured by the ACSM.

In summary, the on average 25 to 30 % difference between the Xact and ICP data can probably be explained by differences in the sampling inlets, the distance between the inlets, and uncertainties of the different analysis methods. The correlation coefficients close to 1 for many elements demonstrate the high precision of the Xact and ICP methods. The obtained time series of those elements can thus reliably be used for source apportionment. The subsequent analyses (e.g., elemental concentration ratios, enhancement ratios) were done with the unmodified Xact data. The only exception is estimation of a mass budget in the discussion of the extreme concentrations in section 3.3.

3.3 Extreme concentrations: the fireworks period

As mentioned in Sect. 3.1 the measurement campaign can be divided into a fireworks and a non-fireworks period. A K concentration > 220 ng m^{-3} served as the criterion to distinguish between these periods, and we required the fireworks period to be contiguous from the first increase in K on 31 July 2015 2200 LT to the final decay to background values on 4 August 2015 1100 LT. The average K concentration during the fireworks period was 2 µg m^{-3}, but this period showed extremely high hourly PM_{10} concentrations and an element mix different from the remainder of our test campaign.

Investigation of the highest peaks reveals the performance of the Xact under high load conditions, when sample thickness may become critical for XRF analysis. A comparison of the two instruments' peaks could demonstrate how closely the Xact mass represents the total measured PM_{10} mass. Inspection of the different time series indicates that the TEOM peak is broader (3 h) and higher (~~59.6~~60 µg m^{-3}), and its maximum concentration is reached 1 h later (at 2 August 2015 0000 LT), but its increase in concentration starts at the same time as the Xact (at 2200 LT). The delay in the maximum can be attributed to the time constant of the TEOM used for reducing measurement noise and to the averaging procedure. For a comparison of the two peaks their measured masses were integrated over the duration of the peaks, i.e., over 2 h for the Xact data and the ACSM data, and 3 h for the NABEL data. The integrated NABEL PM_{10} mass reached a ~~-~~concentration of ~~121.9~~122~~-~~ µg m^{-3}. The Xact 625 monitor reported a total of ~~85.8~~86 µg m^{-3} for the sum of all analysed elements (except Pd, which was used only as an internal standard).

The bulk of this concentration (84~~.3~~ µg m^{-3}) was made up of a few elements (in ~~brackets~~parentheses: concentrations in µg m^{-3}, and abundances relative to total analysed element mass, $PM_{10\text{-element}}$): K (~~48.6~~49, ~~56.6~~57 %), S (21.5, 25~~.1~~ %), Cl (7.4, 8.6 %), Fe (3.2, 3.7 %), Ba (2.1, 2.4 %), Si (1.7, 1.9 %). Absolute K and S concentrations are in good agreement with the values in Drewnick et al. (2006). K likely originated from KNO_3, a basic constituent of black powder (Drewnick et al., 2006; Kong et al., 2015).

The ACSM PM_1 contributed 20.5 µg m^{-3} (17 %) to the aerosol concentration in the fireworks peak.

The comparison of the Xact concentration and the TEOM PM_{10} concentration for the 1 August peak requires taking into account the systematic difference between the Xact and TEOM measurements discussed above, and the fact that the elements are typically not present in elemental but rather in their oxidized form, such that the mass of the latter needs to be included for a quantitative comparison. We therefore estimate a mass budget for the fireworks peak, when the six elements

K, S, Cl, Fe, Ba, and Si comprise the bulk of the total mass. We calculate the ion balance for the positive ions K^+, Fe^{2+}, Ba^{2+}, Si^{2+}, submicron NH_4^+ and negative ions Cl^-, SO_4^{2-}, and submicron NO_3^-. We further add all available components from the NABEL station ($PM_{2.5}$ equivalent black carbon, eBC) and the ACSM (NO_3, NH_4, organic aerosols, but not SO_4, as this is already considered with the S in the Xact data) to the mass balance. Using the measured values of the Xact 625 yields an excess of negative ions of 2.7 %, and a total mass of 141~~.0~~ µg m^{-3}, which overestimates the TEOM value of ~~121.9~~122 µg m^{-3} by 16 %. If Xact concentrations were scaled towards the ICP concentrations with the corresponding regression slopes from Table 1, using for Cl and S the average slope of 1.22 from the other four elements, then the calculation yields an excess of 11 % in positive ions which are then assumed to be neutralized by oxygen. This yields a total mass of 116~~.3~~ µg m^{-3}, which is 4.6 % lower than the TEOM value. Our values are lower limits of the total mass, because the balance is incomplete with respect to relevant elements in the fireworks (e.g., Sr) and other chemical species like carbonaceous and nitrogen containing molecules in the coarse fraction. The result shows that the bulk of fireworks PM_{10} aerosols are a few metals oxidised to sulphates, chlorides, and oxides. Overall, these results further demonstrate the advantage of Xact's high time resolution sampling for associating high metal concentration episodes with source emission activities.

3.4 Investigation of sources

Trace elements can be excellent tracers for specific aerosol sources (e.g., Hopke, 2016; Park et al., 2014; Querol et al., 2007; Visser et al., 2015a). A simple approach for characterizing a common source for a group of elements is to study the temporal covariation of the elements in this group. For our Härkingen data, the time series indicate the strong influence of the fireworks on the concentrations of K, S, Ti, Cu, and Ba (Figures 6 and 7), which are important constituents of fireworks along with Sr as fireworks tracer (Kong et al., 2015; Moreno et al., 2007). Examination of a few raw spectra from the fireworks and non-fireworks periods indeed identified an enhancement of Sr during the fireworks duration, while the peak was definitively absent during the non-fireworks period. Sr was, however, not quantified in our configuration, as we put emphasis on crustal elements and some special trace elements difficult to detect in Switzerland (Hg, Pt).

The 1-hour sampling interval further enabled examination of diurnal variations of the elements. Ca and Ba are presented in Figure 6 and the other elements in the supplement (Fig. S4), which shows the classification of the data according to fireworks and non-fireworks periods. It can be seen for the time from 2300 h to 0600 h that the elements Ba, Bi, Cu, K, S, and Ti show a clear distinction between the two periods. The fireworks elements show a maximum concentration at 2300 LT and a gradual decay over the next 6 to 12 h into the morning hours of the (following) day. Mn, Fe and Zn also show an increased and then decaying concentration after midnight, but the difference compared to non-fireworks days is within the data variability. Si is depleted during the fireworks period relative to the non-fireworks period. This is probably a weekday vs. weekend effect, when fewer heavy duty vehicles (HDV) circulate (Switzerland does not permit HDV use on Sundays), and less road dust is re-suspended (Bukowiecki et al., 2009; 2010). For the non-fireworks cases the transition elements Mn, Fe, Zn, and the element Pb are characterized by a broad morning peak with a maximum around 1000 LT, correlating well with the increasing traffic in the morning hours, and the breakup of the temperature inversion. ~~.~~ It should be pointed out that this observation is consistent with the differences between the Xact and ICP-MS being due to the sampler's closer proximity to the road.

To identify the fireworks tracers, an enhancement ratio (ER) was defined as the ratio between the mean concentrations of an element for the fireworks period to the concentrations in the non-fireworks period (Figure 7). For K, Cu, and Ba the ER is larger than 2 (Cu), and goes up to 10.6 (Ba). S, Cl, Ti, Zn and Pb show an intermediate ER between 1 and 2. Cr, Mn, and Fe ER are close to 1. Si and Ca are depleted with an ER around 0.5, both of which are probably related to the above weekend effect. The elements with the high ER are clearly identified as elements of fireworks: S, K, Ti, Cu, Zn, Ba, Bi.

Further refinement of sources can be obtained when classifying the non-fireworks data by wind direction into a north (270° – 0° - 90°) and a south (90° – 180° - 270°) sector (Figure 8), with the south sector more strongly influenced by highway

emissions (Hueglin et al., 2006). The north sector characterizes the (rural) background concentrations of the central Swiss plateau. Table S1 summarizes the mean element concentrations for the campaign divided into the different periods and wind sectors. Ba, Cr, Cu, Fe, and Mn show the signature of continuous freeway traffic emissions during the day. Pb and Zn show a morning peak only and are well correlated in both sectors. Si, K, Ca, and Ti show another pattern that could reflect the local and regional transport of crustal material partly re-suspended by traffic (south sector), partly originating from the agricultural area north of the freeway.

Figure 9 shows the enhancement ratios south/north. Apart from Cl, all south – north differences are positive, and Si, S, Ca, and Fe concentration differences are larger than 80 ng m^{-3}. These are mainly crustal elements (although Fe is also emitted from vehicles). The enhancement ratios of the transition elements Cr, Mn, Fe, Cu, Zn, Ba, and Pb are larger than 1.2 and related to traffic emissions (engine abrasion, tyre wear, brake wear).

4 Conclusions

A three-week test of a Cooper Environmental Xact 625 Ambient Metals Monitor was performed at the Swiss NABEL station Härkingen. The instrument was configured to measure 24 elements continuously with 1-h time resolution. The selection of elements ranged from Si to Bi, thus covering a range of environmentally relevant elements. Besides the 'standard' elements from K to Pb, which have been well characterized by the manufacturer with respect to their accuracies and detection limits, we included several abundant light elements (Si, S, Cl) and – more for curiosity - some low-concentration elements (As, Pt, Hg) in our selection to test the behaviour of the instrument in a typical Swiss environment. We tested the measurement quality of the Xact 625 by intercomparison with well-established methodologies (ICP-OES and ICP-MS analyses on 24-h PM_{10} samples for major and trace elements, and AuAAA for Hg), ACSM, and TEOM, and used additional meteorological data for the interpretation of the results.

The general findings are:

- The total of elements analysed with the Xact comprised ~~of~~ approximately 20 % of the PM_{10} mass.
- The Xact 625 produced element concentration time series that were highly correlated with the ICP analyses of 24-h filter samples ($r^2 \geq 0.95$), even though the slopes deviated from 1.
- Element concentrations ranged from ng m^{-3} (in background conditions) to tens of µg m^{-3} (during the fireworks), and no instability in operation due to sample overload or else could be observed.
- The m~~M~~easured concentrations agreed reasonably well with other recent field measurements in Switzerland.

The results for measurement accuracy, precision and data quality are:

- Excellent correlation between Xact 625 and ICP-OES/ICP-MS was observed for 24-h averages of the elements S, K, Ca, Ti, Mn, Fe, Cu, Zn, Ba, and Pb ("Group A"). The daily averages calculated from hourly measurements by Xact were on average 30 % higher (range -3 % to +80 %, ~~dependent~~ depending on the element~~s~~) than 24-h integrated filter measurements by ICP. Systematic differences of on average 25 to 30 % could be attributed to physical reasons in the experiment settings, such as the different characteristics of the two inlet systems, the distance between the inlets and to the main source (freeway), and uncertainties in the various analysis methods. For XRF this includes particle size dependent self-absorption effects for the lighter elements and line interferences between different elements. For ICP this includes the entire sampling, digestion and the analysis procedure, as indicated by limited inter-laboratory and inter-method comparisons, as well as the impurities in blank filters). Further research on these issues is needed.
- The accuracy of hourly values has only been tested for the case of the fireworks peak late on 1 August 2015, where the sum of all elements has been compared to the total mass of the NABEL TEOM. Good agreement between the Xact and TEOM mass was found when corrections derived from the 24-h filter analyses were applied. This was a

special case dominated by just three elements, S, K, Cl, and a generalization to all measured elements is not recommended.

- The remaining elements ("Group B") of the filter intercomparison, V, Cr, Co, Ni, As, Se, Cd, Sn, Sb, Hg, and Bi (11 elements) were mostly below detection limit of at least one method, or showed issues with the analysis procedures (Sn, Sb, Hg). A general quantitative statement on their quality could not be achieved. Notice here that a longer sampling time, e.g., 2 or 4 hours, would have lowered the Xact MDLs and therefore increased the number of good measurements, but at the cost of a reduced time resolution.
- Si and Cl were not analysed on the filters, and their Xact detection limits have not yet been determined. Hence their accuracies could not be quantified directly. Some indirect approaches were calculated.
- The Pt concentrations reported by the Xact 625 were below MDL, and Pt was not analysed on the filters. No conclusion about the accuracy of this difficult to measure element can be drawn.

Compared to rotating drum impactor sampling with synchrotron radiation induced XRF or streaker sampling with PIXE analysis, the Xact 625 measures ambient concentrations of the most relevant elements in near real time, and provides data with a delay of only one sampling/analysis cycle. The ~~C~~continuous operation capability of Xact also circumvents the sample number limitations due to restricted beamtime assignments at synchrotrons. This is a major advantage compared to the usual time delay of a couple months caused by the restricted access to synchrotron or accelerator facilities. Of course, the high time resolution of the Xact 625 comes at the cost of sensitivity, visible in the minimum detection limits, which are higher than the MDLs for the offline methods. Xact can be set for longer sampling intervals to extend the number of samples with analysed elements above their MDLs depending on the objective of monitoring campaigns. Xact streamlines near-real time monitoring of multi-metals despite not being as cost effective relative to conventional samplers that could be deployed in larger numbers at many sites simultaneously, or that could sample several size fractions at once, although their actual analysis costs (laboratories, accelerator facilities and staffing needs) are not considered here and they may surmount the instrument costs manifold. Overall, high time resolution sampling of metals provides a rich dataset for associating high metal concentration episodes with source emission activities. Useful extensions of the present capabilities of the Xact could be the addition of more elements to be analysed (especially under the circumstance that the full mix of observed elements cannot always be known in advance), improved quantification of the lightest elements (especially their MDLs), a vacuum or helium device for analysing light elements like Na and Mg, and an inlet switch to alternately measure PM_{10} and $PM_{2.5}$ with one single instrument.

5 Supplementary Material

6 Competing interests

Krag Petterson and Varun Yadav are employed by Cooper Environmental Services, the manufacturer of the Xact® 625.

7 Acknowledgements

This study has been partly funded by the Swiss Federal Office for the Environment (FOEN). M.C. Minguillón acknowledges the Ramón y Cajal Fellowship awarded by the Spanish Ministry of Economy, Industry and Competitiveness. We thank René Richter and Roland Scheidegger of PSI for their support during the field campaign. We are grateful to Chris Koch and John Cooper of Cooper Environmental Services for instructions on instrument operation and numerous discussions on the results. Andrés Alastuey, Xavier Querol and laboratory personnel from IDAEA-CSIC are also acknowledged. We also thank Julie Swift and Randy Mercurio of ERG for the ICP-MS analyses.

8 References

ACES: Equivalence of PM10 instruments at a road traffic site, Stockholm University, Stockholm, Sweden, 67 pp., 2012.

Alastuey, A., Querol, X., Aas, W., Lucarelli, F., Pérez, N., Moreno, T., Cavalli, F., Areskoug, H., Balan, V., Catrambone, M., Ceburnis, D., Cerro, J. C., Conil, S., Gevorgyan, L., Hueglin, C., Imre, K., Jaffrezo, J. L., Leeson, S. R., Mihalopoulos, N., Mitosinkova, M., O'Dowd, C. D., Pey, J., Putaud, J. P., Riffault, V., Ripoll, A., Sciare, J., Sellegri, K., Spindler, G., and Yttri, K. E.: Geochemistry of PM10 over Europe during the EMEP intensive measurement periods in summer 2012 and winter 2013, Atmos. Chem. Phys., 16, 6107-6129, 2016.

Annegarn, H. J., Braga Marcazzan, G. M., Cereda, E., Marchionni, M., and Zucchiatti, A.: Source profiles by unique ratios (SPUR) analysis: Determination of source profiles from receptor-site streaker samples, Atmospheric Environment. Part A. General Topics, 26, 333-343, 1992.

BAFU and Empa: NABEL - Luftbelastung 2014, Bern, Switzerland, UZ-1515-D, 132 pp., 2015.

Botasini, S., Heijo, G., and Méndez, E.: Toward decentralized analysis of mercury (II) in real samples. A critical review on nanotechnology-based methodologies, Anal. Chim. Acta, 800, 1-11, 2013.

Bukowiecki, N., Hill, M., Gehrig, R., Zwicky, C. N., Lienemann, P., Hegedüs, F., Falkenberg, G., Weingartner, E., and Baltensperger, U.: Trace metals in ambient air: Hourly size-segregated mass concentrations determined by synchrotron-XRF, Environ. Sci. Technol., 39, 5754-5762, 2005.

Bukowiecki, N., Lienemann, P., Zwicky, C. N., Furger, M., Richard, A., Falkenberg, G., Rickers, K., Grolimund, D., Borca, C., Hill, M., Gehrig, R., and Baltensperger, U.: X-ray fluorescence spectrometry for high throughput analysis of atmospheric aerosol samples: The benefits of synchrotron X-rays, Spectrochim. Acta, Part B: Atomic Spectroscopy, 63, 929-938, 2008.

Bukowiecki, N., Lienemann, P., Hill, M., Figi, R., Richard, A., Furger, M., Rickers, K., Falkenberg, G., Zhao, Y., Cliff, S. S., Prevot, A. S. H., Baltensperger, U., Buchmann, B., and Gehrig, R.: Real-world emission factors for antimony and other brake wear related trace elements: Size-segregated values for light and heavy duty vehicles, Environ. Sci. Technol., 43, 8072-8078, 2009.

Bukowiecki, N., Lienemann, P., Hill, M., Furger, M., Richard, A., Amato, F., Prévôt, A. S. H., Baltensperger, U., Buchmann, B., and Gehrig, R.: PM10 emission factors for non-exhaust particles generated by road traffic in an urban street canyon and along a freeway in Switzerland, Atmos. Environ., 44, 2330-2340, 2010.

Calzolai, G., Chiari, M., Lucarelli, F., Nava, S., and Portarena, S.: Proton induced γ-ray emission yields for the analysis of light elements in aerosol samples in an external beam set-up, Nucl. Instrum. Methods Phys. Res., Section B: Beam Interactions with Materials and Atoms, 268, 1540-1545, 2010.

Calzolai, G., Lucarelli, F., Chiari, M., Nava, S., Giannoni, M., Carraresi, L., Prati, P., and Vecchi, R.: Improvements in PIXE analysis of hourly particulate matter samples, Nucl. Instrum. Methods Phys. Res., Section B: Beam Interactions with Materials and Atoms, 363, 99-104, 2015.

Chiaradia, M. and Cupelin, F.: Gas-to-particle conversion of mercury, arsenic and selenium through reactions with traffic-related compounds? Indications from lead isotopes, Atmos. Environ., 34, 327-332, 2000.

Crenn, V., Sciare, J., Croteau, P. L., Verlhac, S., Fröhlich, R., Belis, C. A., Aas, W., Äijälä, M., Alastuey, A., Artiñano, B., Baisnée, D., Bonnaire, N., Bressi, M., Canagaratna, M., Canonaco, F., Carbone, C., Cavalli, F., Coz, E., Cubison, M. J., Esser-Gietl, J. K., Green, D. C., Gros, V., Heikkinen, L., Herrmann, H., Lunder, C., Minguillón, M. C., Močnik, G., O'Dowd, C. D., Ovadnevaite, J., Petit, J. E., Petralia, E., Poulain, L., Priestman, M., Riffault, V., Ripoll, A., Sarda-Estève, R., Slowik, J. G., Setyan, A., Wiedensohler, A., Baltensperger, U., Prévôt, A. S. H., Jayne, J. T., and Favez, O.: ACTRIS ACSM intercomparison - Part 1: Reproducibility of concentration and fragment results from 13 individual quadrupole aerosol chemical speciation monitors (Q-ACSM) and consistency with co-located instruments, Atmos. Meas. Tech., 8, 5063-5087, 2015.

Currie, L.: Detection and quantification in X-ray fluorescence spectrometry. In: X-Ray fluorescence analysis of environmental samples, Dzubay, T. G. (Ed.), IX, Ann Arbor Science Publishers, 289-306, 1977.

D'Alessandro, A., Lucarelli, F., Mandò, P. A., Marcazzan, G., Nava, S., Prati, P., Valli, G., Vecchi, R., and Zucchiatti, A.: Hourly elemental composition and sources identification of fine and coarse PM10 particulate matter in four Italian towns, J. Aerosol. Sci., 34, 243-259, 2003.

Diez, S., Montuori, P., Querol, X., and Bayona, J. M.: Total mercury in the hair of children by combustion atomic absorption spectrometry (Comb-AAS), J. Anal. Toxicol., 31, 144-149, 2007.

Drewnick, F., Hings, S. S., Curtius, J., Eerdekens, G., and Williams, J.: Measurement of fine particulate and gas-phase species during the New Year's fireworks 2005 in Mainz, Germany, Atmos. Environ., 40, 4316-4327, 2006.

Escrig, A., Monfort, E., Celades, I., Querol, X., Amato, F., Minguillón, M. C., and Hopke, P. K.: Application of optimally scaled target factor analysis for assessing source contribution of ambient PM10, J. Air Waste Manage. Assoc., 59, 1296-1307, 2009.

Formenti, P., Nava, S., Prati, P., Chevaillier, S., Klaver, A., Lafon, S., Mazzei, F., Calzolai, G., and Chiari, M.: Self-attenuation artifacts and correction factors of light element measurements by X-ray analysis: Implication for mineral dust composition studies, J. Geophys. Res.: Atmos., 115, D01203, 2010.

Gälli Purghart, B. C., Nyffeler, U. P., Schindler, P. W., Van Borm, W. A., and Adams, F. C.: Metals in airborne particulate matter in rural Switzerland, Atmos. Environ., Part A., 24, 2191-2206, 1990.

Gerboles, M., Buzica, D., Brown, R. J. C., Yardley, R. E., Hanus-Illnar, A., Salfinger, M., Vallant, B., Adriaenssens, E., Claeys, N., Roekens, E., Sega, K., Jurasovic, J., Rychlik, S., Rabinak, E., Tanet, G., Passarella, R., Pedroni, V., Karlsson, V., Alleman, L., Pfeffer, U., Gladtke, D., Olschewski, A., O'Leary, B., O'Dwyer, M., Pockeviciute, D., Biel-Cwikowska, J., and Tursic, J.: Interlaboratory comparison exercise for the determination of As, Cd, Ni and Pb in PM10 in Europe, Atmos. Environ., 45, 3488-3499, 2011.

Gianini, M. F. D., Gehrig, R., Fischer, A., Ulrich, A., Wichser, A., and Hueglin, C.: Chemical composition of PM10 in Switzerland: An analysis for 2008/2009 and changes since 1998/1999, Atmos. Environ., 54, 97-106, 2012.

Hagler, G. S. W., Baldauf, R. W., Thoma, E. D., Long, T. R., Snow, R. F., Kinsey, J. S., Oudejans, L., and Gullett, B. K.: Ultrafine particles near a major roadway in Raleigh, North Carolina: Downwind attenuation and correlation with traffic-related pollutants, Atmos. Environ., 43, 1229-1234, 2009.

Hopke, P. K.: Review of receptor modeling methods for source apportionment, J. Air Waste Manage. Assoc., 66, 237-259, 2016.

Hueglin, C., Gehrig, R., Baltensperger, U., Gysel, M., Monn, C., and Vonmont, H.: Chemical characterisation of PM2.5, PM10 and coarse particles at urban, near-city and rural sites in Switzerland, Atmos. Environ., 39, 637-651, 2005.

Hueglin, C., Buchmann, B., and Weber, R. O.: Long-term observation of real-world road traffic emission factors on a motorway in Switzerland, Atmos. Environ., 40, 3696 - 3709, 2006.

Kong, S. F., Li, L., Li, X. X., Yin, Y., Chen, K., Liu, D. T., Yuan, L., Zhang, Y. J., Shan, Y. P., and Ji, Y. Q.: The impacts of firework burning at the Chinese Spring Festival on air quality: insights of tracers, source evolution and aging processes, Atmos. Chem. Phys., 15, 2167-2184, 2015.

Lanz, V. A., Prévôt, A. S. H., Alfarra, M. R., Weimer, S., Mohr, C., DeCarlo, P. F., Gianini, M. F. D., Hueglin, C., Schneider, J., Favez, O., D'Anna, B., George, C., and Baltensperger, U.: Characterization of aerosol chemical composition with aerosol mass spectrometry in Central Europe: an overview, Atmos. Chem. Phys., 10, 10453-10471, 2010.

Lucarelli, F., Nava, S., Calzolai, G., Chiari, M., Udisti, R., and Marino, F.: Is PIXE still a useful technique for the analysis of atmospheric aerosols? The LABEC experience, X-Ray Spectrom., 40, 162-167, 2011.

Lundgren, D. A.: An ~~Aerosol~~ aerosol ~~Sampler~~ sampler for ~~Determination~~ determination of ~~Particle~~ particle ~~Concentration~~ concentration as a ~~Function~~ function of ~~Size~~ size and ~~Time~~time, JAPCA~~Journal of the Air Pollution Control Association~~, 17, 225-229, 1967.

Middlebrook, A. M., Bahreini, R., Jimenez, J. L., and Canagaratna, M. R.: Evaluation of composition-dependent collection efficiencies for the Aerodyne aerosol mass spectrometer using field data, Aerosol Sci. Technol., 46, 258-271, 2012.

Minguillón, M. C., Querol, X., Baltensperger, U., and Prévôt, A. S. H.: Fine and coarse PM composition and sources in rural and urban sites in Switzerland: Local or regional pollution?, Sci. Total Environ., 427–428, 191-202, 2012.

Moreno, T., Querol, X., Alastuey, A., Cruz Minguillón, M., Pey, J., Rodriguez, S., Vicente Miró, J., Felis, C., and Gibbons, W.: Recreational atmospheric pollution episodes: Inhalable metalliferous particles from firework displays, Atmos. Environ., 41, 913-922, 2007.

Ng, N. L., Herndon, S. C., Trimborn, A., Canagaratna, M. R., Croteau, P. L., Onasch, T. B., Sueper, D., Worsnop, D. R., Zhang, Q., Sun, Y. L., and Jayne, J. T.: An aerosol chemical speciation monitor (ACSM) for routine monitoring of the composition and mass concentrations of ambient aerosol, Aerosol Sci. Technol., 45, 780-794, 2011.

Panteliadis, P., Helmink, H. J. P., Koopman, P. C., Hoonhout, M., de Jonge, D., and Visser, J. H.: PM10 sampling inlets comparison: EPA vs EU, European Aerosol Conference, Granada, Spain, 2012.

Park, S.-S., Cho, S. Y., Jo, M. R., Gong, B. J., Park, J. S., and Lee, S. J.: Field evaluation of a near–real time elemental monitor and identification of element sources observed at an air monitoring supersite in Korea, Atmos. Pollut. Res., 5, 119-128, 2014.

Querol, X., Alastuey, A., Rodriguez, S., Plana, F., Ruiz, C. R., Cots, N., Massagué, G., and Puig, O.: PM10 and PM2.5 source apportionment in the Barcelona metropolitan area, Catalonia, Spain, Atmos. Environ., 35, 6407-6419, 2001.

Querol, X., Viana, M., Alastuey, A., Amato, F., Moreno, T., Castillo, S., Pey, J., de la Rosa, J., Sánchez de la Campa, A., Artíñano, B., Salvador, P., García Dos Santos, S., Fernández-Patier, R., Moreno-Grau, S., Negral, L., Minguillón, M. C., Monfort, E., Gil, J. I., Inza, A., Ortega, L. A., Santamaría, J. M., and Zabalza, J.: Source origin of trace elements in PM from regional background, urban and industrial sites of Spain, Atmos. Environ., 41, 7219-7231, 2007.

Querol, X., Pey, J., Minguillón, M. C., Pérez, N., Alastuey, A., Viana, M., Moreno, T., Bernabé, R. M., Blanco, S., Cárdenas, B., Vega, E., Sosa, G., Escalona, S., Ruiz, H., and Artíñano, B.: PM speciation and sources in Mexico during the MILAGRO-2006 campaign, Atmos. Chem. Phys., 8, 111-128, 2008.

Richard, A., Bukowiecki, N., Lienemann, P., Furger, M., Fierz, M., Minguillón, M. C., Weideli, B., Figi, R., Flechsig, U., Appel, K., Prévôt, A. S. H., and Baltensperger, U.: Quantitative sampling and analysis of trace elements in atmospheric aerosols: impactor characterization and synchrotron-XRF mass calibration, Atmos. Meas. Tech., 3, 1473-1485, 2010.

Richard, A., Gianini, M. F. D., Mohr, C., Furger, M., Bukowiecki, N., Minguillón, M. C., Lienemann, P., Flechsig, U., Appel, K., DeCarlo, P. F., Heringa, M. F., Chirico, R., Baltensperger, U., and Prévôt, A. S. H.: Source apportionment of size and time resolved trace elements and organic aerosols from an urban courtyard site in Switzerland, Atmos. Chem. Phys., 11, 8945-8963, 2011.

Röösli, M., Theis, G., Künzli, N., Staehelin, J., Mathys, P., Oglesby, L., Camenzind, M., and Braun-Fahrländer, C.: Temporal and spatial variation of the chemical composition of PM10 at urban and rural sites in the Basel area, Switzerland, Atmos. Environ., 35, 3701-3713, 2001.

Sánchez-Rodas, D., Sánchez de la Campa, A. M., de la Rosa, J. D., Oliveira, V., Gómez-Ariza, J. L., Querol, X., and Alastuey, A.: Arsenic speciation of atmospheric particulate matter (PM10) in an industrialised urban site in southwestern Spain, Chemosphere, 66, 1485-1493, 2007.

Sarmiento, A. M., Oliveira, V., Gómez-Ariza, J. L., Nieto, J. M., and Sánchez-Rodas, D.: Diel cycles of arsenic speciation due to photooxidation in acid mine drainage from the Iberian Pyrite Belt (Sw Spain), Chemosphere, 66, 677-683, 2007.

Visser, S., Slowik, J. G., Furger, M., Zotter, P., Bukowiecki, N., Canonaco, F., Flechsig, U., Appel, K., Green, D. C., Tremper, A. H., Young, D. E., Williams, P. I., Allan, J. D., Coe, H., Williams, L. R., Mohr, C., Xu, L., Ng, N. L., Nemitz, E., Barlow, J. F., Halios, C. H., Fleming, Z. L., Baltensperger, U., and Prévôt, A. S. H.: Advanced source apportionment of size-resolved trace elements at multiple sites in London during winter, Atmos. Chem. Phys., 15, 11291-11309, 2015a.

Visser, S., Slowik, J. G., Furger, M., Zotter, P., Bukowiecki, N., Dressler, R., Flechsig, U., Appel, K., Green, D. C., Tremper, A. H., Young, D. E., Williams, P. I., Allan, J. D., Herndon, S. C., Williams, L. R., Mohr, C., Xu, L., Ng, N. L., Detournay, A., Barlow, J. F., Halios, C. H., Fleming, Z. L., Baltensperger, U., and Prévôt, A. S. H.: Kerb and urban increment of highly time-resolved trace elements in PM10, PM2.5 and PM1.0 winter aerosol in London during ClearfLo 2012, Atmos. Chem. Phys., 15, 2367-2386, 2015b.

Yadav, V. and Turner, J.: Gauging intraurban variability of ambient particulate matter arsenic and other air toxic metals from a network of monitoring sites, Atmos. Environ., 89, 318-328, 2014.

Yatkin, S., Gerboles, M., and Borowiak, A.: Evaluation of standardless EDXRF analysis for the determination of elements on PM10 loaded filters, Atmos. Environ., 54, 568-582, 2012.

Yatkin, S., Belis, C. A., Gerboles, M., Calzolai, G., Lucarelli, F., Cavalli, F., and Trzepla, K.: An interlaboratory comparison study on the measurement of elements in PM10, Atmos. Environ., 125, 61-68, 2016.

~~Yatkin, S., Gerboles, M., and Borowiak, A.: Evaluation of standardless EDXRF analysis for the determination of elements on PM10 loaded filters, Atmos. Environ., 54, 568-582, 2012.~~

9 Figures

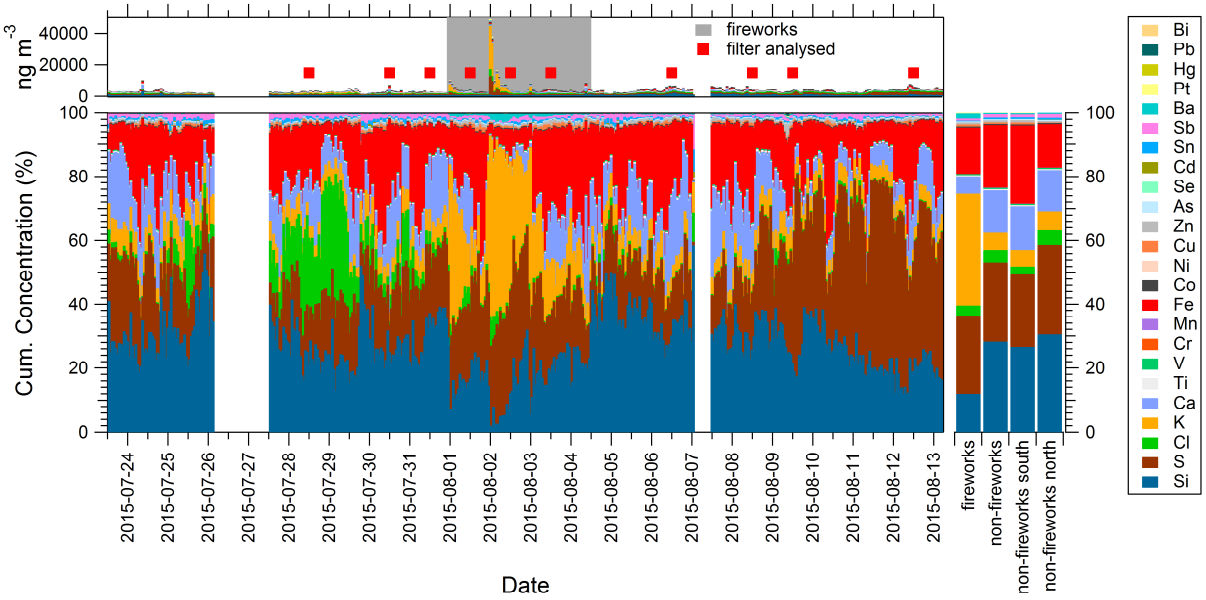

Figure 1: Main panel: Relative amount of analysed elements by Xact 625 during the field campaign. Top panel: Absolute concentrations, stacked. The grey shaded area denotes the fireworks period. The red squares mark the days when 24-h filters were analysed and used for comparisons in this study. Bottom panel: relative cumulative elemental concentrations, stacked. Right panel: Average relative contributions (in %) of elements for the fireworks period, the non-fireworks period, and for the south and north sectors during the non-fireworks period.

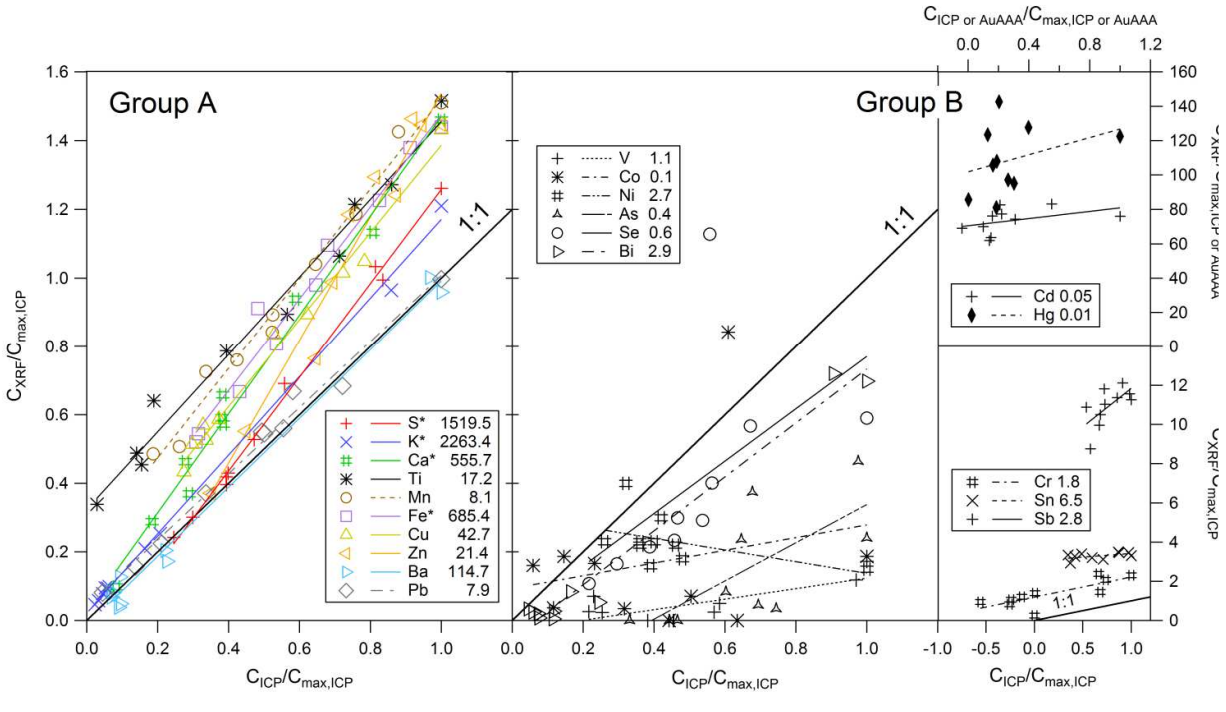

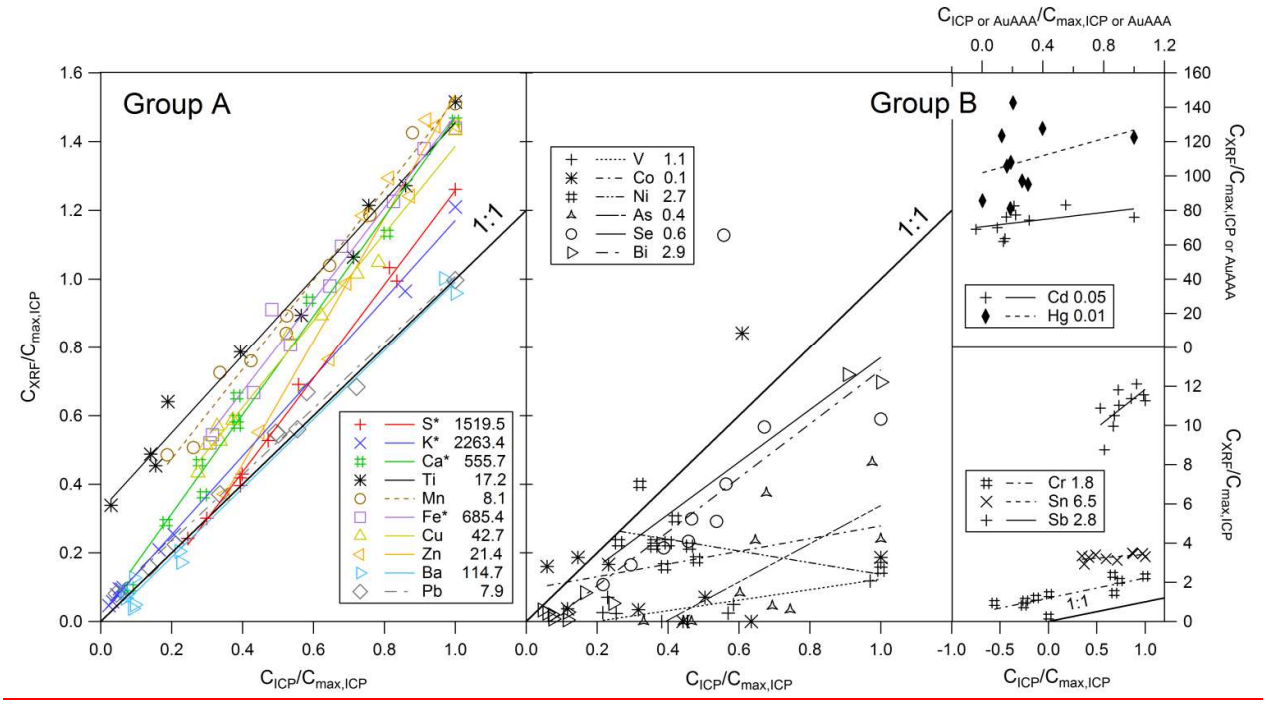

Figure 2: Scatterplots and regression lines of Xact 625 (ordinate) vs. ICP-OES/MS (abscissa) data for Groups A and B. The axes have been scaled by the maximum concentration $C_{max,ICP}$ for each element ($C_{max,AuAAA}$ for Hg). The Levenberg-Marquardt linear least squares fitting method was applied, taking the ICP measurements as the independent data. Regression equation is y = a + bx. See Table 1 for data.

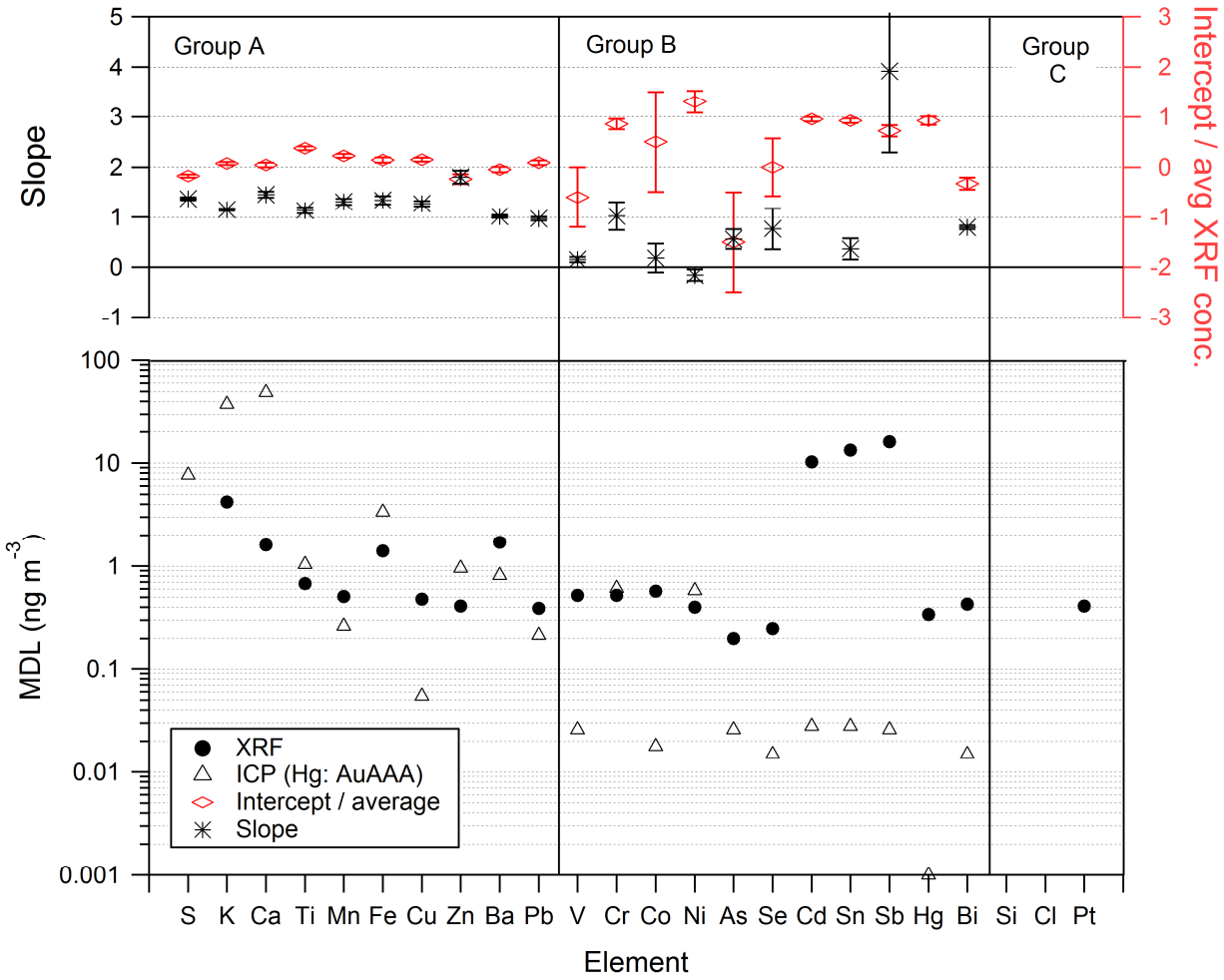

Figure 3: Bottom: Minimum detection limits (MDL), interference free for the Xact 625 (XRF), and for the ICP analyses. Hg was analysed with AuAAA spectrometry. Top: Slopes and intercept ratios (intercepts divided by the average concentrations measured with XRF) with standard deviations for all elements measured with the Xact.

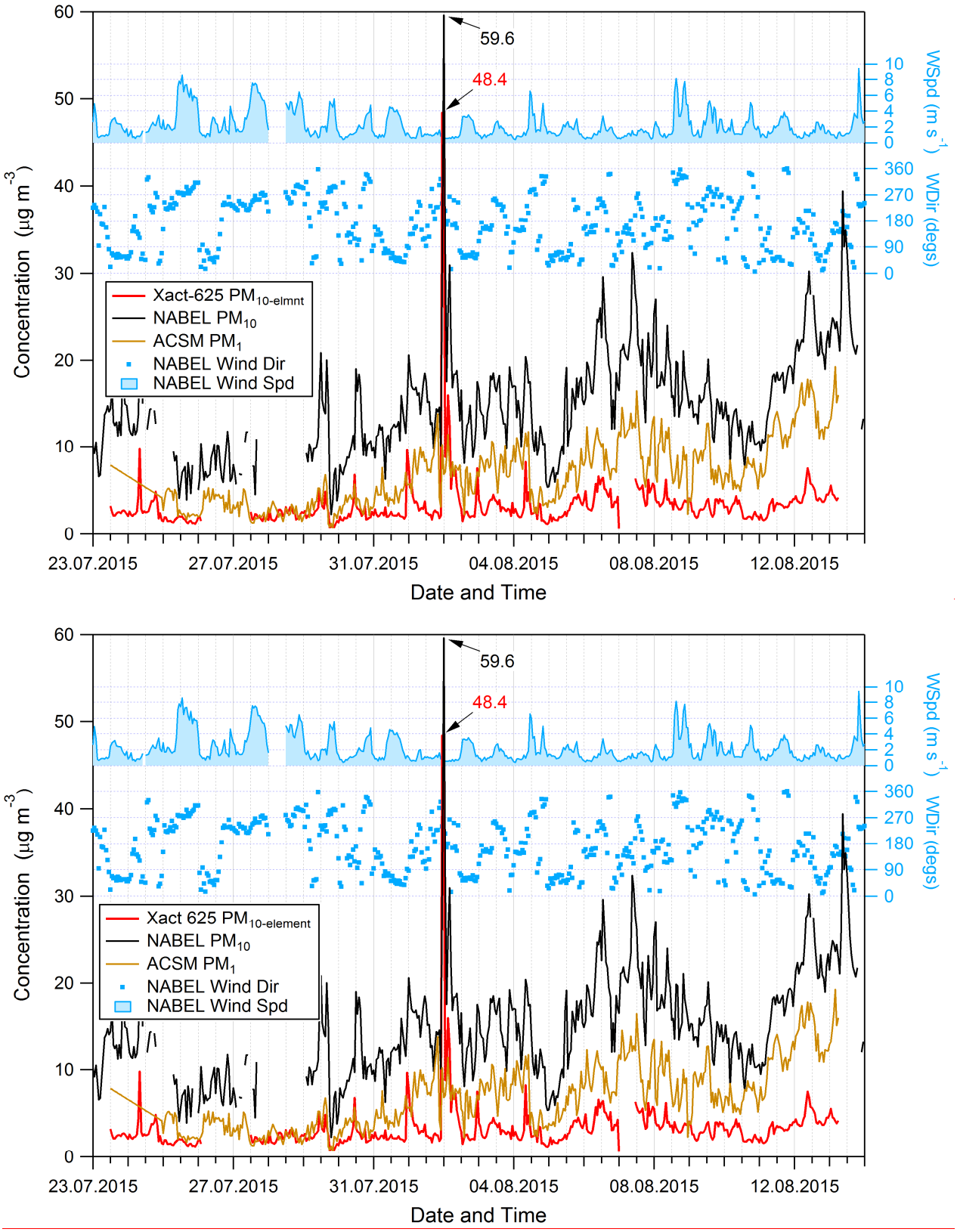

Figure 4: Time series of Xact 625 total elemental concentration, ACSM PM1 data, NABEL TEOM PM_{10} data, and wind speed (WSpd) and direction (WDir) measurements in Härkingen. Numbers at the peaks indicate 1-h concentration maxima.

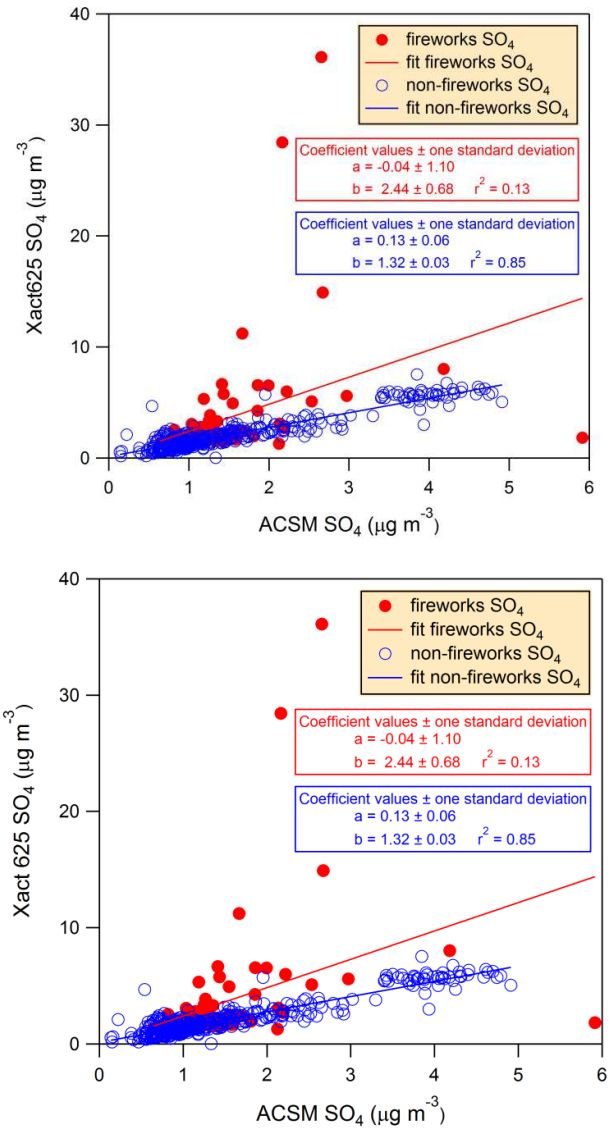

Figure 5: Comparison of Xact PM_{10} SO_4 vs. ACSM PM_1 SO_4. Data were split into fireworks (red) and non-fireworks (blue) periods.

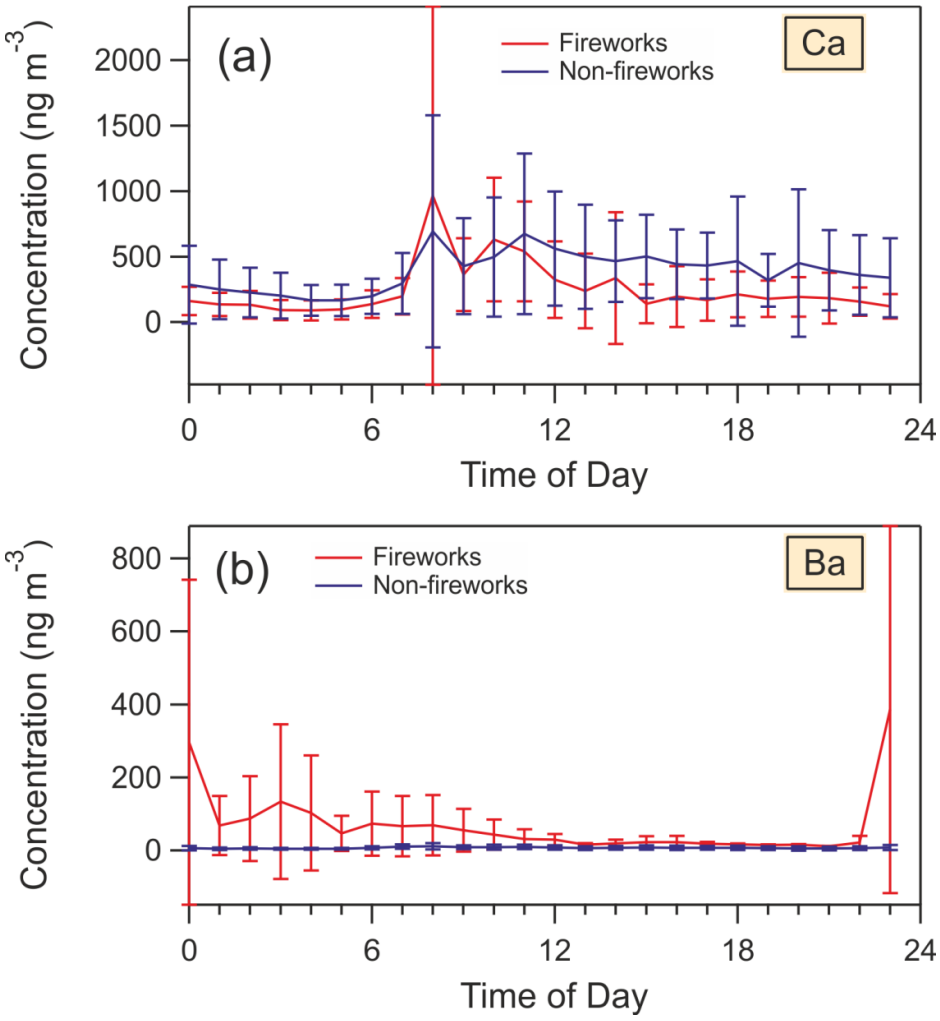

Figure 6: Mean diurnal variations of a) Ca and b) Ba, stratified for fireworks (red) and non-fireworks (blue) periods. Error bars denote ± 1 standard deviation of the averaging period. Diurnal variations for the other elements are shown in the supplement S4 (Fig. S4).

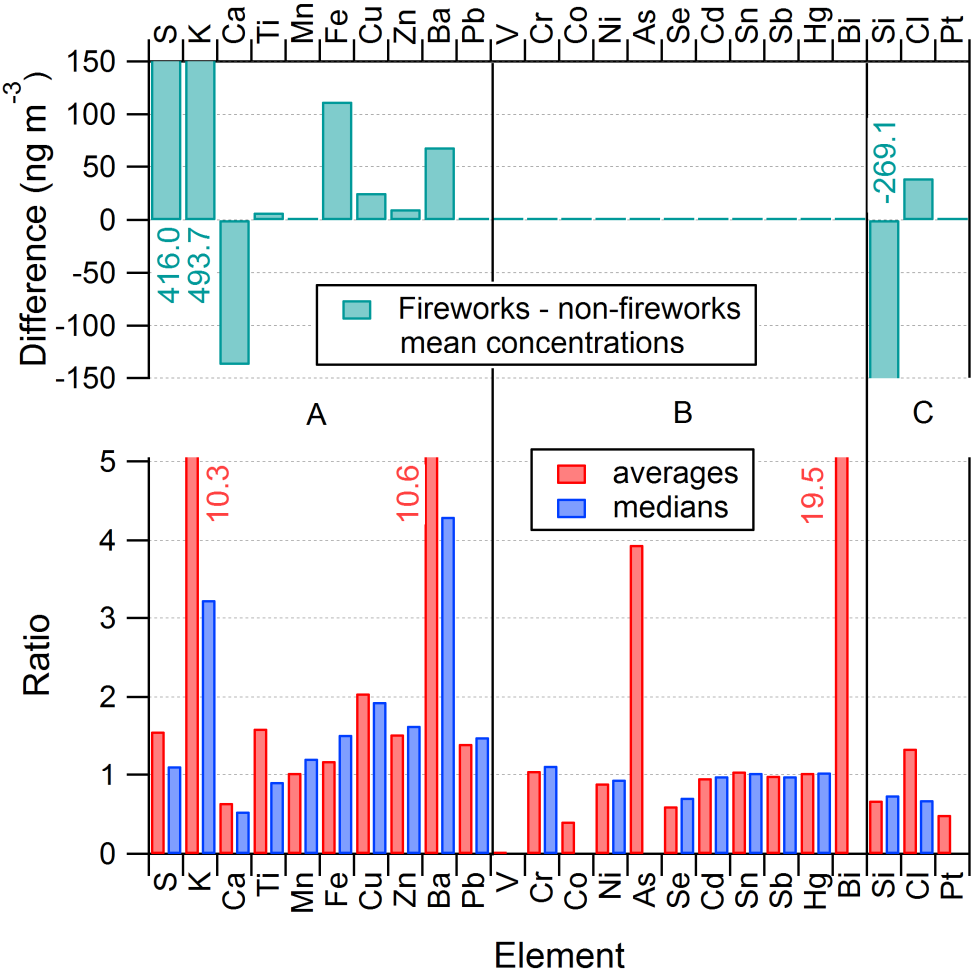

Figure 7: Bottom: Enhancement ratios for all analysed elements for fireworks/non-fireworks classification, sorted by group. Numbers indicate values outside the axis range for S, K, and Si. Top: Difference between average concentrations of fireworks and non-fireworks periods. Numbers indicate values outside the axis range for S, K, and Si (negative).

5

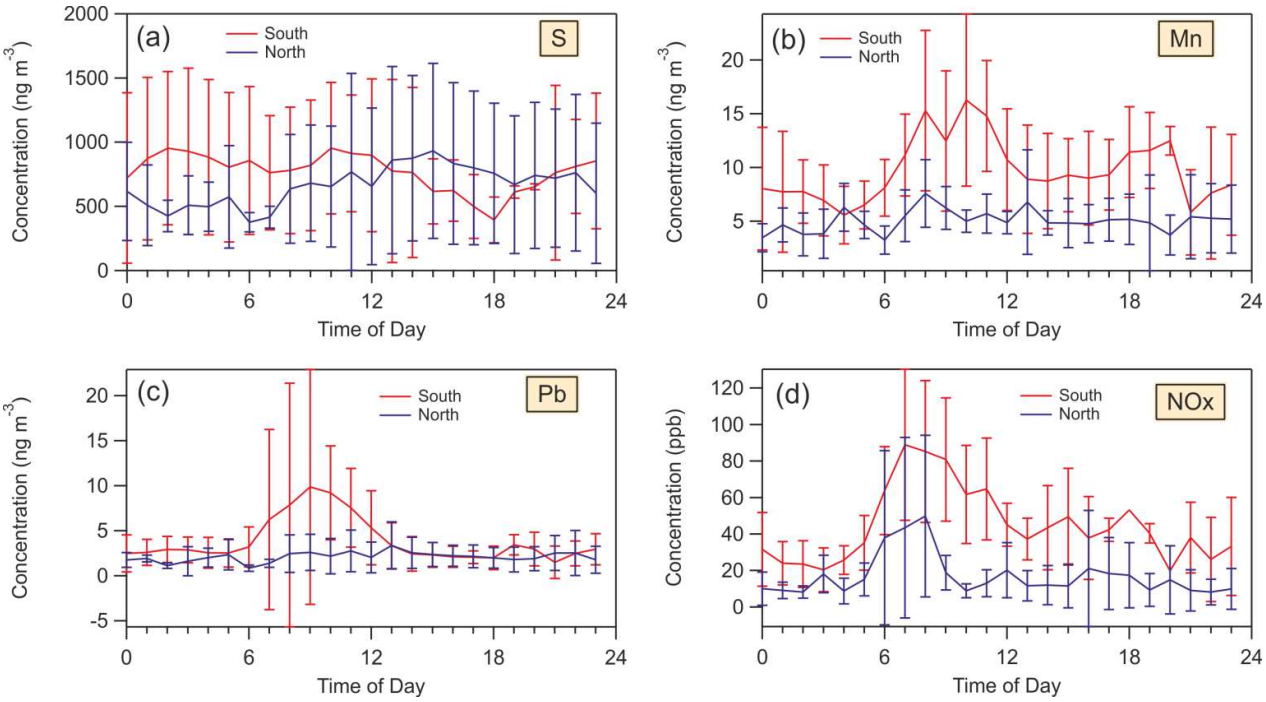

Figure 8: Mean diurnal variations of a) S, b) Mn, c) Pb, and d) NO_x for the non-fireworks period stratified for south and north wind directions. Error bars denote ±1 standard deviation of the averaging period. Diurnal variations for the other elements are shown in the supplement S5 (Fig. S5).

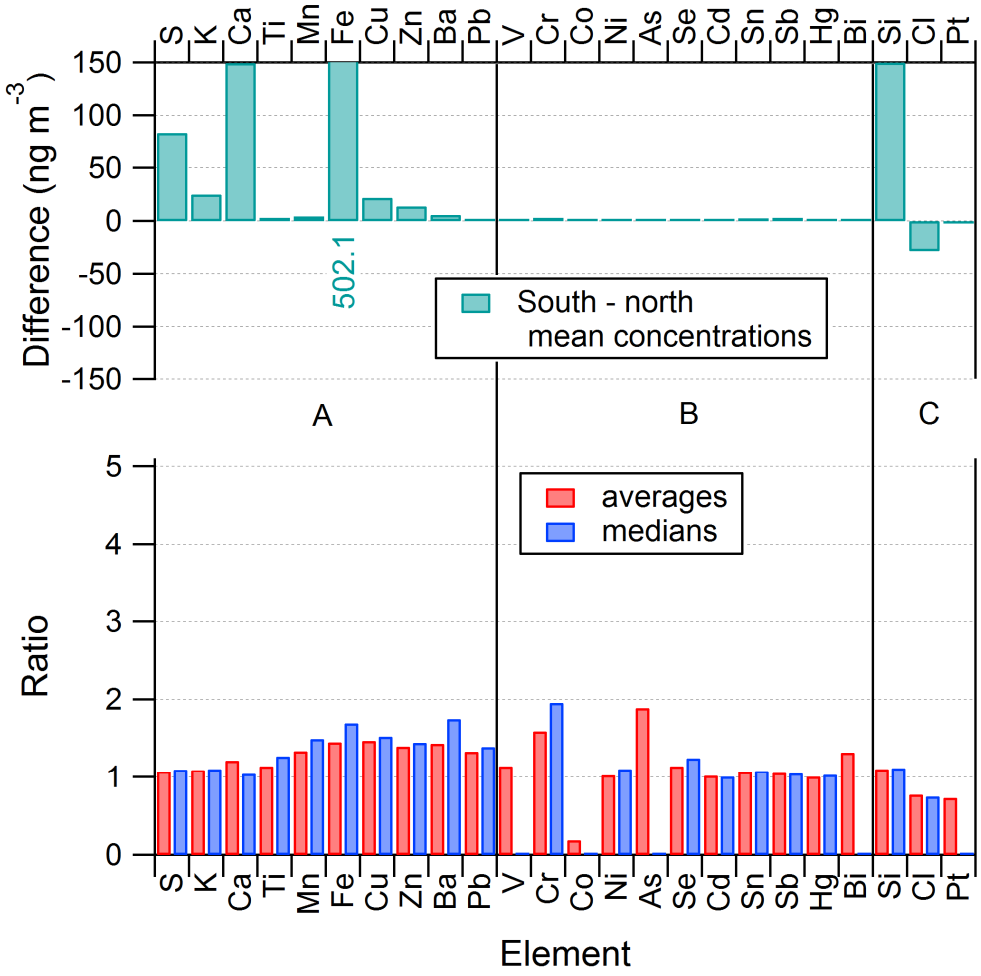

Figure 9: Bottom: Enhancement ratios for all analysed elements for south/north sector classification for the non-fireworks period, sorted by group. Top: 'Background'-subtracted mean concentrations of the south sector for the non-fireworks period. Number indicates value outside the axis range for Fe.

10 Tables

Table 1. Regression coefficients for the comparison of Xact 625 and offline data. The 1-h values of the Xact 625 were averaged to 24-h values. Primed quantities are uncertainties.

			Regression coefficients							Xact		ICP	
Group	Element	Analysis method	fitX = a + bx					Average XRF conc.	Ratio intercept/ average	MDL (60 min)	Pts > MDL	MDL (24 h)	Pts > MDL
			a	± a'	b	± b'	r^2	ng m^{-3}		ng m^{-3}	%	ng m^{-3}	%
A	S	ICP-OES	-170	30.6	1.37	0.03	1.00	956	-0.18			7.7	100
	K	ICP-OES	52.4	19.2	1.15	0.02	1.00	703	0.07	4.20	100	37.8	100
	Ca	ICP-OES	13.9	17.9	1.45	0.06	0.99	365	0.04	1.60	100	49.2	90
	Ti	ICP-MS	5.58	0.57	1.13	0.06	0.98	14.9	0.37	0.68	100	1.04	90
	Mn	ICP-MS	1.72	0.28	1.31	0.06	0.99	7.6	0.23	0.51	100	0.26	100
	Fe	ICP-OES	93.1	35.8	1.34	0.08	0.97	656	0.14	1.40	100	3.4	100
	Cu	ICP-MS	4.93	1.27	1.27	0.05	0.99	33.5	0.15	0.48	100	0.055	100
	Zn	ICP-MS	-5.56	2.18	1.80	0.13	0.96	23.0	-0.24	0.41	100	0.96	100
	Ba	ICP-MS	-1.62	1.73	1.01	0.03	0.99	31.9	-0.05	1.70	94	0.82	100
	Pb	ICP-MS	0.32	0.17	0.97	0.04	0.99	3.8	0.08	0.39	98	0.22	100
B	V	ICP-MS	-0.03	0.03	0.15	0.05	0.57	0.05	-0.62	0.52	2	0.026	100
	Cr	ICP-MS	2.13	0.26	1.02	0.28	0.63	2.5	0.86	0.52	75	0.61	40
	Co	ICP-MS	0.01	0.02	0.18	0.29	0.05	0.02	0.55	0.57	0	0.018	70
	Ni	ICP-MS	0.82	0.14	-0.16	0.11	0.22	0.63	1.31	0.40	68	0.58	100
	As	ICP-MS	-0.09	0.06	0.56	0.20	0.50	0.06	-1.48	0.20	4	0.026	100
	Se	ICP-MS	0.00	0.15	0.76	0.41	0.30	0.26	0.01	0.25	38	0.015	100
	Cd	ICP-MS	6.28	0.28	10.4	7.9	0.18	6.5	0.96	10.3	13	0.028	20
	Sn	ICP-MS	19.7	0.96	0.36	0.21	0.27	21.3	0.93	13.3	85	0.028	100
	Sb	ICP-MS	22.2	3.58	3.9	1.63	0.42	30.6	0.72	16.0	94	0.026	100
	Hg	*Au AAA*	*0.64*	*0.06*	*24.9*	*24.1*	*0.12*	0.69	0.94	0.34	87	*0.001*	*40*
	Bi	ICP-MS	-0.16	0.06	0.79	0.04	0.98	0.49	-0.32	0.43	7	0.015	100
C	Si												
	Cl												
	Pt									0.41	2		
	Group A	average slope			1.28								
	Group A	standard deviation			0.24								

			Regression coefficients							Xact		ICP	
Group	Element	Analysis method	fitX = a + bx					Average XRF conc.	Ratio intercept/ average	MDL (60 min)	Pts > MDL	MDL (24 h)	Pts > MDL
			a	± a'	b	± b'	r^2	ng m^{-3}		ng m^{-3}	%	ng m^{-3}	%
A	S	ICP-OES	-169.73	30.57	1.37	0.03	1.00	956.48	-0.177			7.662	100
	K	ICP-OES	52.42	19.15	1.15	0.02	1.00	703.47	0.075	4.20	100.00	37.808	100
	Ca	ICP-OES	13.87	17.91	1.45	0.06	0.99	365.41	0.038	1.60	100.00	49.195	90
	Ti	ICP-MS	5.58	0.57	1.13	0.06	0.98	14.94	0.373	0.68	100.00	1.043	90
	Mn	ICP-MS	1.72	0.28	1.31	0.06	0.99	7.59	0.227	0.51	100.00	0.264	100
	Fe	ICP-OES	93.05	35.80	1.34	0.08	0.97	656.22	0.142	1.40	100.00	3.398	100
	Cu	ICP-MS	4.93	1.27	1.27	0.05	0.99	33.49	0.147	0.48	100.00	0.055	100
	Zn	ICP-MS	-5.56	2.18	1.80	0.13	0.96	22.97	-0.242	0.41	100.00	0.959	100
	Ba	ICP-MS	-1.62	1.73	1.01	0.03	0.99	31.92	-0.051	1.70	94.30	0.819	100
	Pb	ICP-MS	0.32	0.17	0.97	0.04	0.99	3.84	0.085	0.39	98.20	0.216	100
B	V	ICP-MS	-0.03	0.03	0.15	0.05	0.57	0.05	-0.619	0.52	2.00	0.026	100
	Cr	ICP-MS	2.13	0.26	1.02	0.28	0.63	2.48	0.860	0.52	74.60	0.614	40
	Co	ICP-MS	0.01	0.02	0.18	0.29	0.05	0.02	0.555	0.57	0.44	0.018	70
	Ni	ICP-MS	0.82	0.14	-0.16	0.11	0.22	0.63	1.310	0.40	67.80	0.581	100
	As	ICP-MS	-0.09	0.06	0.56	0.20	0.50	0.06	-1.481	0.20	4.00	0.026	100
	Se	ICP-MS	0.00	0.15	0.76	0.41	0.30	0.26	0.015	0.25	38.00	0.015	100
	Cd	ICP-MS	6.28	0.28	10.37	7.86	0.18	6.54	0.960	10.30	12.70	0.028	20
	Sn	ICP-MS	19.73	0.96	0.36	0.21	0.27	21.29	0.927	13.30	85.00	0.028	100
	Sb	ICP-MS	22.17	3.58	3.92	1.63	0.42	30.60	0.724	16.00	94.00	0.026	100
	Hg	*Au AAA*	*0.64*	*0.06*	*24.88*	*24.13*	*0.12*	0.69	0.935	0.34	86.80	*0.001*	*40*
	Bi	ICP-MS	-0.16	0.06	0.79	0.04	0.98	0.49	-0.318	0.43	7.20	0.015	100
C	Si												
	Cl												
	Pt									0.41	1.75		
	Group A	average slope			1.28								
	Group A	standard deviation			0.24								

Table 2. Comparison of Xact data with published ICP data of other campaigns.

Group		Xact 625 averages	Filter samples								
		Non-fireworks days	Belp	Geneva	Basel, summer	Payerne	Zürich	Zürich, summer	Payerne, summer	Payerne, summer	Härkingen NABEL
	Reference		1)	2)	3)	4)	5)	6)	6)	7)	8)
	# cases, size	17	PM8	PM10	PM10	PM10	PM10	PM10	PM10	PM10	PM10
	Sampling period	2015	1985/86	1996/97	1997/98	1998/99	2008/09	2009	2009	2012	2015
	Unit	ng/m³	ng/m³	ng/m³	ng/m³	ng/m³	ng/m³	ng/m³	ng/m³	ng/m³	ng/m³
A	S	790					2394	625	637	360	
	K	167			630	98	1318	187	188	120	
	Ca	398			720	100	137	451	355	180	
	Ti	11.3			38		6.5	13.9	14.3	9.9	
	Mn	7.2	31.7		16	2.8	5.8	7.2	5	2.8	
	Fe	594			760	89	390	455	202	130	
	Cu	24.4	7.9	35	75	6	28.1	17.4	4.3	2.8	19.7
	Zn	19.0	65.0	120	73		20.3	16.1	9.4	7.5	
	Ba	7.1			110		6.7	6.5	3.9	1.8	
	Pb	3.0	134	95	51	10	14.2	3.6	3.1	1.2	4.9
B	V	0.06	3.9			0.7	0.4	1.0	1.2	0.7	
	Cr	2.4			8		0.9	2.3	1.6	1.0	
	Co	0.02					2.6	0.1	0.1		
	Ni	0.63			8	1.2	0.6	0.9	1.0	0.5	0.9
	As	0.02	2.2	2	1	0.53		0.3	0.5	0.2	0.31
	Se	0.30		6		0.16		0.3	0.3	0.2	
	Cd	6.7	0.88	0.4	0	0.32		0.1	0.1		0.07
	Sn	20.9					2.6	2.6	1.0		
	Sb	31.6			29	0.26	2.5	2.4	0.5		
	Hg	0.64		0.5							
	Bi	0.07						0.2	0.1		
C	Si	829					211	571	634	370	
	Cl	109			41		657	66	190	30	
	Pt	0.05									

1)	Gälli Purghart et al. 1990
2)	Chiaradia and Cupelin 2000 - fortnight averages
3)	Röösli et al. 2001
4)	Hueglin et al. 2005
5)	Richard et al. 2011
6)	Minguillón et al. 2012
7)	Alastuey et al. 2016
8)	BAFU/Empa 2015 - annual mean values

	Xact 625 averages		Switzerland								
	All days	Non-fireworks days	Belp	Geneva	Basel, summer	Payerne	Zürich	Zürich, summer	Payerne, summer	Payerne, summer	Härkingen NABEL
Reference			1)	2)	3)	4)	5)	6)	6)	7)	8)
# cases, size	22	17	PM8	PM10	PM10	PM10	PM10	PM10	PM10	PM10	PM10
Sampling period	2015	2015	1985/86	1996/97	1997/98	1998/99	2008/09	2009	2009	2012	2015
Unit	ng/m³	ng/m³	ng/m³	ng/m³	ng/m³	ng/m³	ng/m³	ng/m³	ng/m³	ng/m³	ng/m³
Si	783.14	829.45					210.90	571.00	634.00	370.00	
S	822.74	790.19					2394.30	625.00	637.00	360.00	
Cl	113.17	109.40			41.00		656.50	66.00	190.00	30.00	
K	408.00	166.56			630.00	98.00	1318.20	187.00	188.00	120.00	
Ca	367.99	397.57			720.00	100.00	137.40	451.00	355.00	180.00	
Ti	12.26	11.30			38.00		6.50	13.90	14.30	9.90	
V	0.05	0.06	3.90			0.70	0.40	1.00	1.20	0.70	
Cr	2.39	2.43			8.00		0.90	2.30	1.60	1.00	
Mn	7.11	7.21	31.70		16.00	2.80	5.80	7.20	5.00	2.80	
Fe	600.48	593.92			760.00	89.00	389.70	455.00	202.00	130.00	
Co	0.01	0.02					2.60	0.10	0.10		
Ni	0.60	0.63			8.00	1.20	0.60	0.90	1.00	0.50	0.90
Cu	28.04	24.45	7.90	35.00	75.00	6.00	28.10	17.40	4.30	2.80	19.70
Zn	20.23	19.04	65.00	120.00	73.00		20.30	16.10	9.40	7.50	
As	0.03	0.02	2.20	2.00	1.00	0.53		0.30	0.50	0.20	0.31
Se	0.27	0.30		6.00		0.16		0.30	0.30	0.20	
Cd	6.57	6.67	0.88	0.40	0.00	0.32		0.10	0.10		0.07
Sn	21.00	20.93					2.60	2.60	1.00		
Sb	31.33	31.59			29.00	0.26	2.50	2.40	0.50		
Ba	18.09	7.12			110.00		6.70	6.50	3.90	1.80	
Pt	0.04	0.05									
Hg	0.64	0.64		0.50							
Pb	3.13	3.04	134.00	95.00	51.00	10.00	14.20	3.60	3.10	1.20	4.90
Bi	0.26	0.07						0.20	0.10		

1)	Gälli et al. 1990
2)	Chiaradia and Cupelin 2000 - fortnight averages
3)	Röösli et al. 2001
4)	Hueglin et al. 2005
5)	Richard et al. 2011
6)	Minguillón et al. 2012
7)	Alastuey et al. 2016
8)	BAFU/Empa 2015 - annual mean values

S1. General statistics of Xact 625 data

Table S1: Data characteristics of Xact 625 measurements in Härkingen. Elements are sorted according to the groups in Table 21). Data were classified into fireworks and non-fireworks periods. The non-fireworks period was further classified into north (rural) and south (freeway) sectors according to the wind direction. Numbers in italics indicate cases where the daily averages were <MDL. The cases for the two wind sectors do not add up to the non-fireworks cases as wind data are missing for a total of 12 h (cf. Fig. 1).

	Non-Fireworks				Fireworks				South sector (non-fireworks)				North sector (non-fireworks)			
Element	avg	sdev	max	median	avg	sdev	max	median	avg	sdev	max	median	avg	sdev	max	median
	ng m^{-3}	ng m^{-3}	ng m^{-3}	ng m^{-3}	ng m^{-3}	ng m^{-3}	ng m^{-3}	ng m^{-3}	ng m^{-3}	ng m^{-3}	ng m^{-3}	ng m^{-3}	ng m^{-3}	ng m^{-3}	ng m^{-3}	ng m^{-3}
# cases	370				86				173				185			
S	739	525	2508	602	1155	1667	12034	677	795	516	2254	660	712	537	2508	499
K	161	57	484	153	1661	3855	27349	494	176	61	395	169	151	50	484	145
Ca	391	385	3211	263	253	390	3109	141	474	476	3211	275	325	266	2254	253
Ti	11.4	8.1	43.4	8.8	18.3	36.2	282.2	8.0	13.1	8.9	39.6	11.1	10.3	7.2	43.4	8.2
Mn	7.1	4.6	27.0	5.7	7.3	3.9	22.2	7.0	9.5	5.1	27.0	8.6	5.0	2.8	21.0	4.7
Fe	587	429	2338	460	700	386	1909	700	852	453	2338	780	350	228	1309	304
Cu	24.1	17.7	109	20.1	49.3	48.7	372	38.9	35.5	18.3	109	30.7	13.5	8.5	49.0	9.9
Zn	18.7	16.8	143	14.3	28.6	18.9	104	23.4	26.1	20.8	143	20.7	12.3	8.0	66.1	10.7
Ba	7.1	5.5	25.3	5.3	75.4	169	1127	22.6	10.2	6.0	25.3	9.2	4.4	3.2	17.2	3.5
Pb	3.0	3.9	41.1	2.0	4.2	3.0	15.3	3.0	3.9	5.3	41.1	2.8	2.2	1.6	9.4	1.7
V	*0.06*	*0.15*	*1.22*	*0.00*	*0.00*	*0.00*	*0.00*	*0.00*	*0.07*	*0.18*	*1.22*	*0.00*	*0.05*	*0.13*	*0.89*	*0.00*
Cr	2.4	2.3	13	1.75	2.5	2.2	9.2	1.98	3.8	2.5	13	3.4	1.09	1.10	6.2	0.76
Co	*0.02*	*0.08*	*0.70*	*0.00*	*0.01*	*0.03*	*0.23*	*0.00*	*0.00*	*0.02*	*0.21*	*0.00*	*0.03*	*0.11*	*0.70*	*0.00*
Ni	0.62	0.65	10.3	0.54	0.56	0.35	1.95	0.51	0.64	0.45	4.0	0.59	0.61	0.81	10.3	0.50
As	*0.02*	*0.14*	*1.31*	*0.00*	*0.09*	*0.31*	*1.91*	*0.00*	*0.04*	*0.20*	*1.31*	*0.00*	*0.01*	*0.06*	*0.84*	*0.00*
Se	*0.27*	*0.32*	*4.4*	*0.20*	*0.16*	*0.13*	*0.44*	*0.14*	*0.30*	*0.41*	*4.4*	*0.24*	*0.24*	*0.22*	*0.90*	*0.17*
Cd	*6.8*	*3.6*	*23.6*	*6.2*	*6.5*	*3.1*	*21.3*	*6.1*	*6.9*	*3.7*	*19.1*	*6.3*	*6.7*	*3.6*	*23.6*	*6.2*
Sn	20.8	7.8	55.3	19.6	21.8	8.3	54.3	20.1	22.1	8.4	55.3	21.1	19.6	7.0	45.4	18.7
Sb	31.3	11.2	112	29.8	31.0	10.4	68.0	29.4	33.0	11.9	77.6	31.3	29.9	10.4	112	28.9
Hg	0.63	0.25	1.49	0.61	0.64	0.18	1.31	0.63	0.63	0.23	1.18	0.63	0.64	0.26	1.49	0.61
Bi	*0.07*	*0.12*	*0.70*	*0.00*	*1.27*	*3.8*	*23.5*	*0.15*	*0.09*	*0.13*	*0.50*	*0.00*	*0.04*	*0.10*	*0.70*	*0.00*
Si	839	398	3415	714	570	224	1758	532	925	469	3415	796	775	309	2052	682
Cl	114	200	970	26.4	153	578	4455	18.1	88.0	161	871	19.8	116	211	970	30.5
Pt	*0.05*	*0.11*	*0.66*	*0.00*	*0.03*	*0.07*	*0.34*	*0.00*	*0.04*	*0.10*	*0.66*	*0.00*	*0.06*	*0.11*	*0.64*	*0.00*

	Non-Fireworks				Fireworks				South sector (non-fireworks)				North sector (non-fireworks)			
Element	avg	sdev	max	median	avg	sdev	max	median	avg	sdev	max	median	avg	sdev	max	median
	ng m^{-3}	ng m^{-3}	ng m^{-3}	ng m^{-3}	ng m^{-3}	ng m^{-3}	ng m^{-3}	ng m^{-3}	ng m^{-3}	ng m^{-3}	ng m^{-3}	ng m^{-3}	ng m^{-3}	ng m^{-3}	ng m^{-3}	ng m^{-3}
# cases	370				86				173				185			
S	739.28	524.59	2508.00	601.85	1155.32	1666.73	12034.00	677.15	795.31	516.19	2254.00	659.85	711.53	537.04	2508.00	499.31
K	161.00	56.98	484.09	152.81	1661.10	3854.66	27349.00	493.69	175.80	60.89	395.34	168.66	150.75	50.00	484.09	144.98
Ca	390.66	384.69	3211.00	262.79	253.21	389.74	3109.00	140.82	474.39	476.21	3211.00	274.58	324.91	266.10	2254.00	252.85
Ti	11.44	8.12	43.38	8.79	18.29	36.16	282.23	8.04	13.08	8.90	39.56	11.14	10.33	7.17	43.38	8.23
Mn	7.10	4.62	26.98	5.72	7.30	3.88	22.21	6.99	9.51	5.14	26.98	8.56	5.03	2.79	20.99	4.71
Fe	587.41	428.85	2338.00	460.08	699.95	385.97	1909.00	699.78	852.36	452.72	2338.00	779.67	350.25	227.50	1309.00	303.58
Cu	24.07	17.69	109.34	20.07	49.28	48.72	371.81	38.91	35.46	18.29	109.34	30.66	13.52	8.55	49.01	9.94
Zn	18.67	16.84	143.37	14.31	28.56	18.94	104.12	23.42	26.13	20.82	143.37	20.67	12.27	7.97	66.14	10.70
Ba	7.12	5.49	25.33	5.25	75.39	169.25	1127.00	22.58	10.19	5.96	25.33	9.19	4.42	3.21	17.22	3.46
Pb	2.96	3.89	41.07	1.99	4.17	3.02	15.30	2.96	3.95	5.26	41.07	2.77	2.18	1.62	9.38	1.72
V	*0.06*	*0.15*	*1.22*	*0.00*	*0.00*	*0.00*	*0.00*	*0.00*	*0.07*	*0.18*	*1.22*	*0.00*	*0.05*	*0.13*	*0.89*	*0.00*
Cr	2.40	2.30	12.96	1.75	2.51	2.22	9.23	1.98	3.81	2.47	12.96	3.43	1.09	1.10	6.17	0.76
Co	*0.02*	*0.08*	*0.70*	*0.00*	*0.01*	*0.03*	*0.23*	*0.00*	*0.00*	*0.02*	*0.21*	*0.00*	*0.03*	*0.11*	*0.70*	*0.00*
Ni	0.62	0.65	10.32	0.54	0.56	0.35	1.95	0.51	0.64	0.45	3.99	0.59	0.61	0.81	10.32	0.50
As	*0.02*	*0.14*	*1.31*	*0.00*	*0.09*	*0.31*	*1.91*	*0.00*	*0.04*	*0.20*	*1.31*	*0.00*	*0.01*	*0.06*	*0.84*	*0.00*
Se	*0.27*	*0.32*	*4.39*	*0.20*	*0.16*	*0.13*	*0.44*	*0.14*	*0.30*	*0.41*	*4.39*	*0.24*	*0.24*	*0.22*	*0.90*	*0.17*
Cd	*6.75*	*3.61*	*23.62*	*6.25*	*6.49*	*3.14*	*21.33*	*6.14*	*6.89*	*3.74*	*19.10*	*6.28*	*6.70*	*3.55*	*23.62*	*6.20*
Sn	20.79	7.82	55.34	19.57	21.78	8.27	54.28	20.10	22.15	8.38	55.34	21.15	19.64	7.01	45.41	18.68
Sb	31.31	11.22	111.88	29.80	30.97	10.42	67.96	29.38	33.03	11.93	77.63	31.30	29.90	10.43	111.88	28.90
Hg	0.63	0.25	1.49	0.61	0.64	0.18	1.31	0.63	0.63	0.23	1.18	0.63	0.64	0.26	1.49	0.61
Bi	*0.07*	*0.12*	*0.70*	*0.00*	*1.27*	*3.82*	*23.47*	*0.15*	*0.09*	*0.13*	*0.50*	*0.00*	*0.04*	*0.10*	*0.70*	*0.00*
Si	839.20	398.20	3415.00	713.75	570.13	223.75	1758.00	532.28	924.98	468.79	3415.00	795.77	775.17	308.86	2052.00	682.42
Cl	113.70	200.20	969.80	26.44	153.07	578.02	4455.00	18.11	87.95	161.12	871.19	19.79	116.38	210.81	969.80	30.50
Pt	*0.05*	*0.11*	*0.66*	*0.00*	*0.03*	*0.07*	*0.34*	*0.00*	*0.04*	*0.10*	*0.66*	*0.00*	*0.06*	*0.11*	*0.64*	*0.00*

S2. Ambient filter samples for method intercomparisons

A quarter each of three NABEL filters of the series analysed at IDAEA were also analysed with XRF at CES and with ICP-MS at ERG. This allows for an intercomparison between benchtop XRF and ICP-MS, between ICP-MS of two different laboratories, and between Xact XRF and benchtop XRF. The elements Zn, Sr, Cu, Pb, Fe, K, Ca, Mn, Se, and Ba were selected for this comparison. Benchtop XRF required no further sample preparation except punching a 47-mm piece of the

original filter. IDAEA's digestion protocol is described in the main paper. Of three different filter blanks, blank 1 appeared contaminated and was not further considered, blanks 2 and 3 were averaged and subtracted from the analysis, but the values are not reported. ERG followed a protocol of the USEPA describing the multi-elemental determination of total metals by ICP-MS in ambient air samples collected on 47 mm Teflon® filters following guidelines in EPA method IO-3.5 and EPA FEM Method "Standard Operating Procedure for the Determination of Lead in PM10 by Inductively Coupled Plasma Mass Spectrometry (ICPMS) with Hot Block Dilute Acid and Hydrogen Peroxide Filter Extraction" (EQL-0512-202). The filters were digested in a HotBlock™ for 2.5 hours using an extraction fluid containing 1.85 % nitric acid (HNO_3), 0.5 % hydrochloric acid (HCl), and 0.17 % hydrofluoric acid (HF) with 0.33 mg/ L^{-1} of gold added for mercury stabilization. One aliquot of hydrogen peroxide (H_2O_2) was added after 1.5 hours of extraction and was allowed to effervesce. The extract was analyzed by ICP-MS and the data were collected using the manufacturer's software. The results are given in Table ~~S1~~S2.

Table S2. Analyses of three ambient (NABEL) samples (1, 6 and 12 August 2015) from Härkingen. Comparisons of Xact and benchtop XRF (CES), benchtop XRF (CES) and ICP-MS (IDAEA and ERG), and ICP-MS at two laboratories (IDAEA and ERG). NR = not reported; BD = below limit of detection.

Sample	Element	Xact Daily Average (ng m^{-3})	CES XRF Results (ng m^{-3})	Background (ng cm^{-2})	IDAEA Results (ng m^{-3})	ERG Values (ng m^{-3})	Background (ng m^{-3})	% Difference							
								CES vs. IDAEA (CES - IDAEA) / IDAEA	Average CES vs. IDAEA	CES vs. ERG (CES - ERG) / ERG	Average CES vs. ERG	ERG vs. IDAEA (ERG - IDAEA) / IDAEA	Average ERG vs IDAEA	Xact vs. CES (Xact-CES)/CES	Average Xact vs. CES
Field_PSI_213	Zn	31	19.2	1.0	19.6	22	64	-1.9	-1.5	-14.2	-0.8	14.4	0.4	62	59
Field_PSI_218		25	16.5	1.0	15.8	15.9	64	4.2		3.5		0.7		54	
Field_PSI_224		30	18.8	1.0	20	17.4	64	-6.7		8.2		-13.7		61	
Field_PSI_213	Sr	NR	60	0.0	61	59	0.9	-1.9	-37	2.4	-32	-4.1	-8.3	NR	NR
Field_PSI_218		NR	1.5	0.0	2.0	1.9	0.9	-24		-18.4		-6.8		NR	
Field_PSI_224		NR	0.2	0.0	1.1	0.9	0.9	-84		-81		-14.0		NR	
Field_PSI_213	Cu	58	45	0.0	42	50	1.9	5.5	-0.1	-10.6	-15.2	18.0	18	31	51
Field_PSI_218		39	26	0.0	26	31	1.9	-1.3		-17.6		20		51	
Field_PSI_224		36	21	0.0	22	26	1.9	-4.5		-17.3		15.5		70	
Field_PSI_213	Pb	4.4	NR	0.0	4.4	4.5	8.7	NR	NR	NR	NR	2.2	-15	NR	NR
Field_PSI_218		4.3	NR	0.0	4.0	3.4	8.7	NR		NR		-15.5		NR	
Field_PSI_224		5.3	NR	0.0	4.6	3.2	8.7	NR		NR		-31		NR	
Field_PSI_213	Fe	757	530	34	465	479	75	13.8	12.4	10.5	9.7	3.0	2.5	43	36
Field_PSI_218		1021	805	33	685	732	75	17.5		10.0		6.9		27	
Field_PSI_224		907	662	33	625	610	75	5.9		8.5		-2.4		37	
Field_PSI_213	K	2641	2046	0.0	2263	2663	41	-9.6	9.7	-23	0.3	17.7	9.9	29	33
Field_PSI_218		226	194	0.0	143	156	41	36		24		9.4		16.3	
Field_PSI_224		210	137	0.0	133	137	41	2.8		0.0		2.8		53	
Field_PSI_213	Ca	214	172	12.9	161	796	190	7.2	4.7	-78	-28	395	136	24	39
Field_PSI_218		792	598	12.6	556	603	190	7.6		-0.9		8.5		32	
Field_PSI_224		518	325	12.7	327	337	190	-0.7		-3.6		3.0		59	
Field_PSI_213	Mn	7.3	8.3	0.1	4.3	5.8	1.4	95	57	42	26	37	25	-12.2	3.4
Field_PSI_218		12.3	11.9	0.1	8.1	9.7	1.4	47		23		19.6		3.1	
Field_PSI_224		11.1	9.3	0.1	7.1	8.4	1.4	31		12		17.3		19.3	
Field_PSI_213	Se	BD	BD	0.0	0.3	0.5	0.1	NR	169	NR	-13.3	64	105	NR	-25
Field_PSI_218		0.3	BD	0.0	0.4	0.5	0.1	NR		NR		41		NR	
Field_PSI_224		0.7	1.0	0.0	0.4	1.1	0.1	169		-13.3		210		-25	
Field_PSI_213	Ba	109	89	13.6	111	111	81	-19.8	-19.8	-19.9	-19.9	0.1	-33	23	23
Field_PSI_218		14.3	BD	13.3	10.7	8.5	81	NR		NR		-21		NR	
Field_PSI_224		9.2	BD	13.3	8.6	1.8	81	NR		NR		-79		NR	

Sample	Element	Xact Daily Average (ng m^{-3})	CES XRF Results (ng m^{-3})	Background (ng cm^{-2})	IDAEA Results (ng m^{-3})	ERG Values (ng m^{-3})	Background (ng m^{-3})	% Difference							
								CES vs. IDAEA (CES - IDAEA) / IDAEA	Average CES vs. IDAEA	CES vs. ERG (CES - ERG) / ERG	Average CES vs. ERG	ERG vs. IDAEA (ERG - IDAEA) / IDAEA	Average ERG vs IDAEA	Xact vs. CES (Xact-CES)/CES	Average Xact vs. CES
Field_PSI_213	Zn	31.2	19.2	1.0	19.6	22.4	64.0	-1.9	-1.5	-14.2	-0.8	14.4	0.4	62.1	59.2
Field_PSI_218		25.4	16.5	1.0	15.8	15.9	64.0	4.2		3.5		0.7		53.9	
Field_PSI_224		30.4	18.8	1.0	20.2	17.4	64.0	-6.7		8.2		-13.7		61.4	
Field_PSI_213	Sr	NR	60.0	0.0	61.1	58.6	0.9	-1.9	-36.6	2.4	-32.5	-4.1	-8.3	NR	NR
Field_PSI_218		NR	1.5	0.0	2.0	1.9	0.9	-23.9		-18.4		-6.8		NR	
Field_PSI_224		NR	0.2	0.0	1.1	0.9	0.9	-84.0		-81.4		-14.0		NR	
Field_PSI_213	Cu	58.2	44.6	0.0	42.2	49.9	1.9	5.5	-0.1	-10.6	-15.2	18.0	17.8	30.5	50.6
Field_PSI_218		39.1	25.8	0.0	26.1	31.3	1.9	-1.3		-17.6		19.8		51.5	
Field_PSI_224		35.8	21.1	0.0	22.1	25.5	1.9	-4.5		-17.3		15.5		69.7	
Field_PSI_213	Pb	4.4	NR	0.0	4.4	4.5	8.7	NR	NR	NR	NR	2.2	-14.8	NR	NR
Field_PSI_218		4.3	NR	0.0	4.0	3.4	8.7	NR		NR		-15.5		NR	
Field_PSI_224		5.3	NR	0.0	4.6	3.2	8.7	NR		NR		-31.1		NR	
Field_PSI_213	Fe	757.1	529.7	33.6	465.5	479.4	74.9	13.8	12.4	10.5	9.7	3.0	2.5	42.9	35.6
Field_PSI_218		1021.1	805.4	32.8	685.4	732.4	74.9	17.5		10.0		6.9		26.8	
Field_PSI_224		906.6	661.6	32.9	624.7	609.7	74.9	5.9		8.5		-2.4		37.0	
Field_PSI_213	K	2640.7	2046.1	0.0	2263.0	2663.0	41.2	-9.6	9.7	-23.2	0.3	17.7	9.9	29.1	32.9
Field_PSI_218		225.8	194.2	0.0	143.0	156.4	41.2	35.8		24.2		9.4		16.3	
Field_PSI_224		209.5	136.7	0.0	133.0	136.7	41.2	2.8		0.0		2.8		53.2	
Field_PSI_213	Ca	213.5	172.1	12.9	160.6	795.5	190.0	7.2	4.7	-78.4	-27.6	395.4	135.6	24.1	38.6
Field_PSI_218		791.9	597.8	12.6	555.7	602.9	190.0	7.6		-0.9		8.5		32.5	
Field_PSI_224		517.9	324.9	12.7	327.2	336.9	190.0	-0.7		-3.6		3.0		59.4	
Field_PSI_213	Mn	7.3	8.3	0.1	4.3	5.8	1.4	94.7	57.5	42.3	25.5	36.9	24.6	-12.2	3.4
Field_PSI_218		12.3	11.9	0.1	8.1	9.7	1.4	46.9		22.8		19.6		3.1	
Field_PSI_224		11.1	9.3	0.1	7.1	8.4	1.4	30.9		11.5		17.3		19.3	
Field_PSI_213	Se	BD	BD	0.0	0.3	0.5	0.1	NR	168.8	NR	-13.3	64.0	105.1	NR	-25.5
Field_PSI_218		0.3	BD	0.0	0.4	0.5	0.1	NR		NR		41.3		NR	
Field_PSI_224		0.7	1.0	0.0	0.4	1.1	0.1	168.8		-13.3		210.0		-25.5	
Field_PSI_213	Ba	109.1	88.9	13.6	110.9	111.0	81.1	-19.8	-19.8	-19.9	-19.9	0.1	-33.2	22.7	22.7
Field_PSI_218		14.3	BD	13.3	10.7	8.5	81.1	NR		NR		-20.5		NR	
Field_PSI_224		9.2	BD	13.3	8.6	1.8	81.1	NR		NR		-79.0		NR	

The data shows a somewhat better comparison between offline XRF and ICP than between online XRF (Xact) and ICP, though the scatter in the relative differences (XRF-ICP/ICP) varied from -37 % (Sr) to +57 % (Mn), if Se and Ba, for which only one filter shows concentrations above the XRF detection limit, are not considered. Comparing the ICP-MS results between the two labs (ERG-IDAEA/IDAEA) shows a range from -33 % (Ba) to +25 % (Mn), when Se and Ca are not considered. Se concentrations are close to their ICP MDL and hence rather uncertain, while Ca shows a problem with one ERG measurement. If Ca and Se are excluded, the average relative difference between the two labs is -0.1 –%, with a standard deviation of 19 –%. Similarly the agreement between each of the labs and bench top XRF is good as well. If Se and Ca are excluded the average percent difference between XRF and IDEA is 5.4 % while the difference between XRF and

ERG is -3.1 %. The comparison of the daily averaged Xact values with the benchtop XRF values shows an average difference of 37 –% (Xact-CES)/CES) for the elements Zn, Cu, Fe, K, Ca, and Mn, which is close to the observed mean difference to ICP. It is also consistent in the sense that all average differences Xact – CES for these elements are positive. The benchtop XRF and the Xact are typically within 5 % when analysing the same standard. Further both benchtop XRF and Xact use the same type of fitting routine (with minor differences in the determination of spectral background), hence the most likely explanation for the difference between the Xact and the labs is differences due to sampling or sampling location.

S3. Spiked filter samples for method intercomparisons

CES produced a set of six quartz filters coated with known amounts of the elements Zn, Sr, Cu, Pb, and Fe. These filters were analysed with a benchtop XRF instrument by CES, and three each of them were sent to IDAEA-CSIC, and ERG for analysis with ICP-MS. The results are presented in Table ~~S2~~S3. Notice that Pb is not reported for XRF, because of large variations of the measured values for quartz filters. This indicates a problem with the XRF fitting routine for quartz filters, as the issue is not seen with Teflon filters.

Table S3. Spiked filter analyses for five elements. Comparison between XRF and ICP-MS analyses performed at three independent laboratories.

Sample Start Time	Sample	Element	CES			IDAEA	ERG		% Difference					Average Percent Difference				
			Spiked Conc. (ng cm^{-2})	XRF Conc. (ng cm^{-2})	Blank (ng cm^{-2})	Conc. (ng cm^{-2})	ERG Values (ng cm^{-2})	Blank (ng cm^{-2})	Spiked vs. CES (CES - spiked) / spiked	Spiked vs. IDAEA (IDAEA - spiked) / spiked	Spiked vs. ERG (ERG - spiked) / spiked	IDAEA vs. CES (CES - IDAEA) / IDAEA	ERG vs. CES (CES - ERG) / ERG	Spiked vs. CES (CES - spiked) / spiked	Spiked vs. IDAEA (IDAEA - spiked) / spiked	Spiked vs. ERG (ERG - spiked) / spiked	IDAEA vs. CES (CES - IDAEA) / IDAEA	ERG vs. CES (CES - ERG) / ERG
21.04.2016 11:50	PQ042116A	Zn	97	88	10.2	133			-9.6	37		-34		-9.7	32	22	-30	-25
21.04.2016 12:25	PQ042116B		97	89	10.2	155			-8.4	59		-42						
21.04.2016 13:00	PQ042116C		97	84	10.2	98			-14	0.3		-14.5						
21.04.2016 15:13	PQ042116D		97	88	10.2		104	31	-9.3		6.8		-15.1					
21.04.2016 15:46	PQ012116E		97	92	10.2		123	31	-5.1		26		-25					
21.04.2016 16:19	PQ042116F		102	90	10.2		136	31	-11		34		-34					
21.04.2016 11:50	PQ042116A	Sr	206	192		179			-7.0	-13.3		7.3		-6.2	-15.7	-7.0	12.7	0.8
21.04.2016 12:25	PQ042116B		206	194		194			-5.8	-5.6		-0.2						
21.04.2016 13:00	PQ042116C		206	194		148			-5.9	-28		31						
21.04.2016 15:13	PQ042116D		206	192			191	1.5	-7.0		-7.5		0.5					
21.04.2016 15:46	PQ012116E		206	194			190	1.5	-5.8		-7.9		2.2					
21.04.2016 16:19	PQ042116F		206	194			195	1.5	-5.9		-5.5		-0.3					
21.04.2016 11:50	PQ042116A	Cu	128	108		112			-15.3	-12.3		-3.4		-13.6	-17.0	5.8	5.9	-18.2
21.04.2016 12:25	PQ042116B		128	111		118			-13.3	-7.7		-6.1						
21.04.2016 13:00	PQ042116C		128	112		88			-12.3	-31		27						
21.04.2016 15:13	PQ042116D		128	108	0.8		131	1.3	-15.3		2.8		-17.6					
21.04.2016 15:46	PQ012116E		128	111	0.8		129	1.3	-13.3		1.4		-14.5					
21.04.2016 16:19	PQ042116F		128	112	0.8		144	1.3	-12.3		13.1		-22					
21.04.2016 11:50	PQ042116A	Pb	21	NR		23			NR	10.3		NR		NR	32	58	NR	NR
21.04.2016 12:25	PQ042116B		21	NR		38			NR	85		NR						
21.04.2016 13:00	PQ042116C		21	NR		21			NR	2.1		NR						
21.04.2016 15:13	PQ042116D		21	NR			27	1.1	NR		32		NR					
21.04.2016 15:46	PQ012116E		21	NR			29	1.1	NR		42		NR					
21.04.2016 16:19	PQ042116F		21	NR			41	1.1	NR		99		NR					
21.04.2016 11:50	PQ042116A	Fe	3025	2760		2828			-8.8	-6.5		-2.4		-8.1	-3.6	-0.8	-2.1	-7.2
21.04.2016 12:25	PQ042116B		3025	2795		3544			-7.6	17.2		-21						
21.04.2016 13:00	PQ042116C		3025	2786		2378			-7.9	-21		17.2						
21.04.2016 15:13	PQ042116D		3025	2760	155		2901	141	-8.8		-4.1		-4.9					
21.04.2016 15:46	PQ012116E		3025	2795	155		2901	141	-7.6		-4.1		-3.6					
21.04.2016 16:19	PQ042116F		3025	2786	155		3203	141	-7.9		5.9		-13.0					

Sample Start Time	Sample	Element	CES			IDAEA	ERG		% Difference					Average Percent Difference				
			Spiked Conc. (ng cm^{-2})	XRF Conc. (ng cm^{-2})	Blank (ng cm^{-2})	Conc. (ng cm^{-2})	ERG Values (ng cm^{-2})	Blank (ng cm^{-2})	Spiked vs. CES (CES - spiked) / spiked	Spiked vs. IDAEA (IDAEA - spiked) / spiked	Spiked vs. ERG (ERG - spiked) / spiked	IDAEA vs. CES (CES - IDAEA) / IDAEA	ERG vs. CES (CES - ERG) / ERG	Spiked vs. CES (CES - spiked) / spiked	Spiked vs. IDAEA (IDAEA - spiked) / spiked	Spiked vs. ERG (ERG - spiked) / spiked	IDAEA vs. CES (CES - IDAEA) / IDAEA	ERG vs. CES (CES - ERG) / ERG
21.04.2016 11:50	PQ042116A	Zn	97.4	88.1	10.2	133.1			-9.6	36.6		-33.8		-9.7	32.0	22.4	-30.3	-24.6
21.04.2016 12:25	PQ042116B		97.4	89.2	10.2	155.0			-8.4	59.1		-42.4						
21.04.2016 13:00	PQ042116C		97.4	83.5	10.2	97.7			-14.3	0.3		-14.5						
21.04.2016 15:13	PQ042116D		97.4	88.3	10.2		104.1	30.7	-9.3		6.8		-15.1					
21.04.2016 15:46	PQ012116E		97.4	92.4	10.2		123.2	30.7	-5.1		26.4		-25.0					
21.04.2016 16:19	PQ042116F		101.5	90.2	10.2		136.0	30.7	-11.2		34.0		-33.7					
21.04.2016 11:50	PQ042116A	Sr	206.0	191.6		178.6			-7.0	-13.3		7.3		-6.2	-15.7	-7.0	12.7	0.8
21.04.2016 12:25	PQ042116B		206.0	194.0		194.5			-5.8	-5.6		-0.2						
21.04.2016 13:00	PQ042116C		206.0	193.9		147.8			-5.9	-28.2		31.1						
21.04.2016 15:13	PQ042116D		206.0	191.6			190.5	1.5	-7.0		-7.5		0.5					
21.04.2016 15:46	PQ012116E		206.0	194.0			189.8	1.5	-5.8		-7.9		2.2					
21.04.2016 16:19	PQ042116F		206.0	193.9			194.6	1.5	-5.9		-5.5		-0.3					
21.04.2016 11:50	PQ042116A	Cu	127.6	108.1		111.9			-15.3	-12.3		-3.4		-13.6	-17.0	5.8	5.9	-18.2
21.04.2016 12:25	PQ042116B		127.6	110.6		117.8			-13.3	-7.7		-6.1						
21.04.2016 13:00	PQ042116C		127.6	111.9		87.9			-12.3	-31.1		27.2						
21.04.2016 15:13	PQ042116D		127.6	108.1	0.8		131.2	1.3	-15.3		2.8		-17.6					
21.04.2016 15:46	PQ012116E		127.6	110.6	0.8		129.4	1.3	-13.3		1.4		-14.5					
21.04.2016 16:19	PQ042116F		127.6	111.9	0.8		144.3	1.3	-12.3		13.1		-22.5					
21.04.2016 11:50	PQ042116A	Pb	20.5	NR		22.6			NR	10.3		NR		NR	32.4	57.7	NR	NR
21.04.2016 12:25	PQ042116B		20.5	NR		37.9			NR	84.7		NR						
21.04.2016 13:00	PQ042116C		20.5	NR		20.9			NR	2.1		NR						
21.04.2016 15:13	PQ042116D		20.5	NR			27.1	1.1	NR		32.0		NR					
21.04.2016 15:46	PQ012116E		20.5	NR			29.1	1.1	NR		41.8		NR					
21.04.2016 16:19	PQ042116F		20.5	NR			40.9	1.1	NR		99.4		NR					
21.04.2016 11:50	PQ042116A	Fe	3024.6	2759.6		2827.6			-8.8	-6.5		-2.4		-8.1	-3.6	-0.8	-2.1	-7.2
21.04.2016 12:25	PQ042116B		3024.6	2795.5		3543.9			-7.6	17.2		-21.1						
21.04.2016 13:00	PQ042116C		3024.6	2786.4		2377.9			-7.9	-21.4		17.2						
21.04.2016 15:13	PQ042116D		3024.6	2759.6	154.5		2901.2	140.5	-8.8		-4.1		-4.9					
21.04.2016 15:46	PQ012116E		3024.6	2795.5	154.5		2901.2	140.5	-7.6		-4.1		-3.6					
21.04.2016 16:19	PQ042116F		3024.6	2786.4	154.5		3202.9	140.5	-7.9		5.9		-13.0					

Tests with specifically produced reference samples of Fe, Cu, Zn, Sr, and Pb (Table ~~S2~~S3) showed relative differences between the measured concentrations and the theoretically expected concentrations ranging from -6.2 % (Sr) to -13.6 % (Cu) for benchtop XRF, on average -9.4 % (without Pb). For all these elements, XRF underestimated the expected value, as expected for absorption of fluorescence radiation by the quartz fiber material (Tanner et al., 1974). Similarly spiked teflon filters (not shown) also showed underestimation of the expected concentrations, though not as much as for the quartz filters. A statistical analysis revealed that at the 99 % confidence level only Cu showed a significant difference between the two filter types. ICP showed differences between -17 % and +32 % (average 5.6 %) for IDAEA-CSIC, and -7 % and +58 % (average 15.6 %) for ERG for quartz filters. The scatter is much larger than for the field samples, and differences can be positive or negative.

S4. Diurnal variations of elements for fireworks and non-fireworks periods

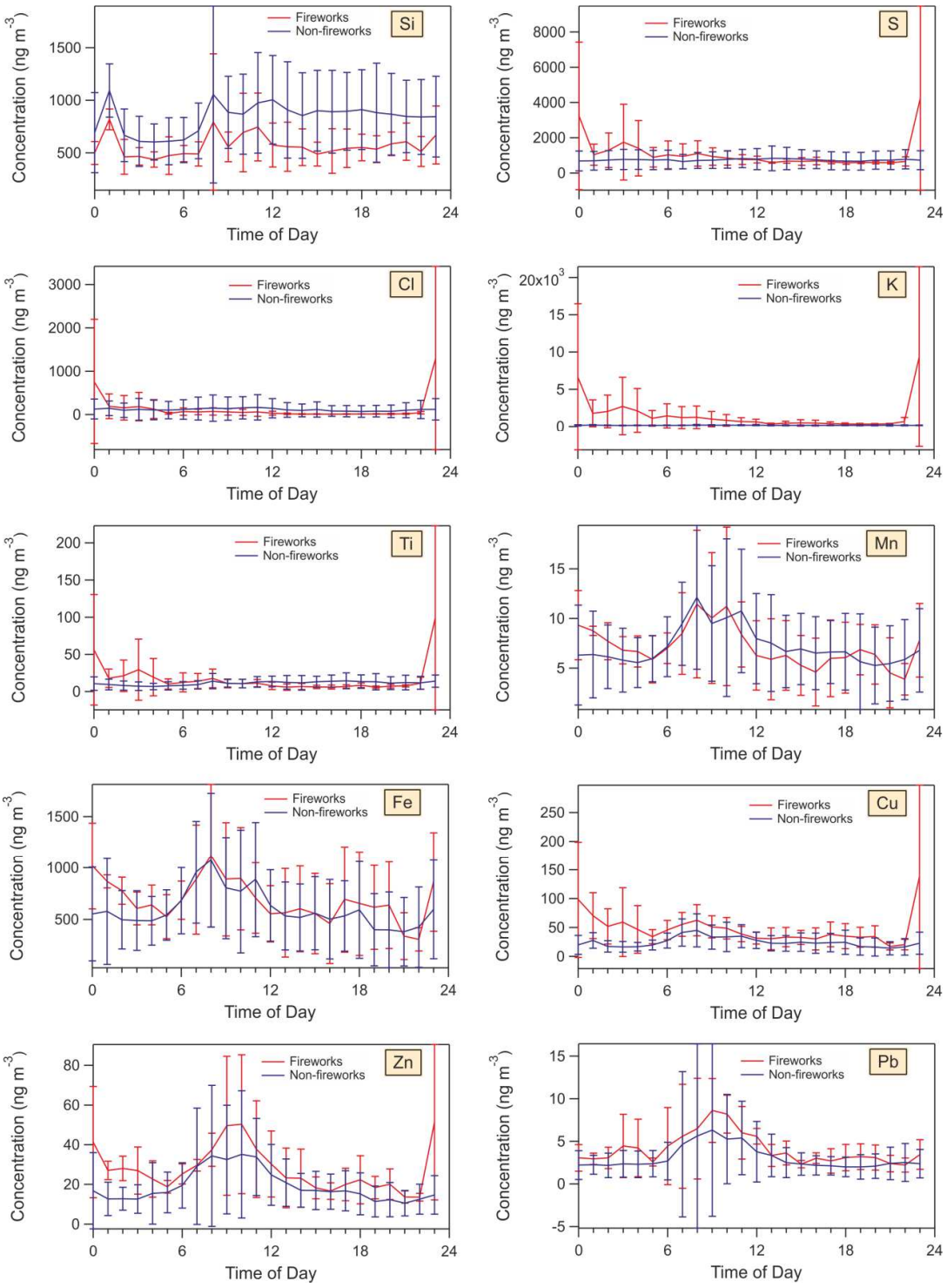

Figure S4: Diurnal variations of the Group A elements Si, S, Cl, K, Ti, Mn, Fe, Cu, Zn, and Pb. See Fig. 6.

S5. Diurnal variations of elements for north and south wind sectors

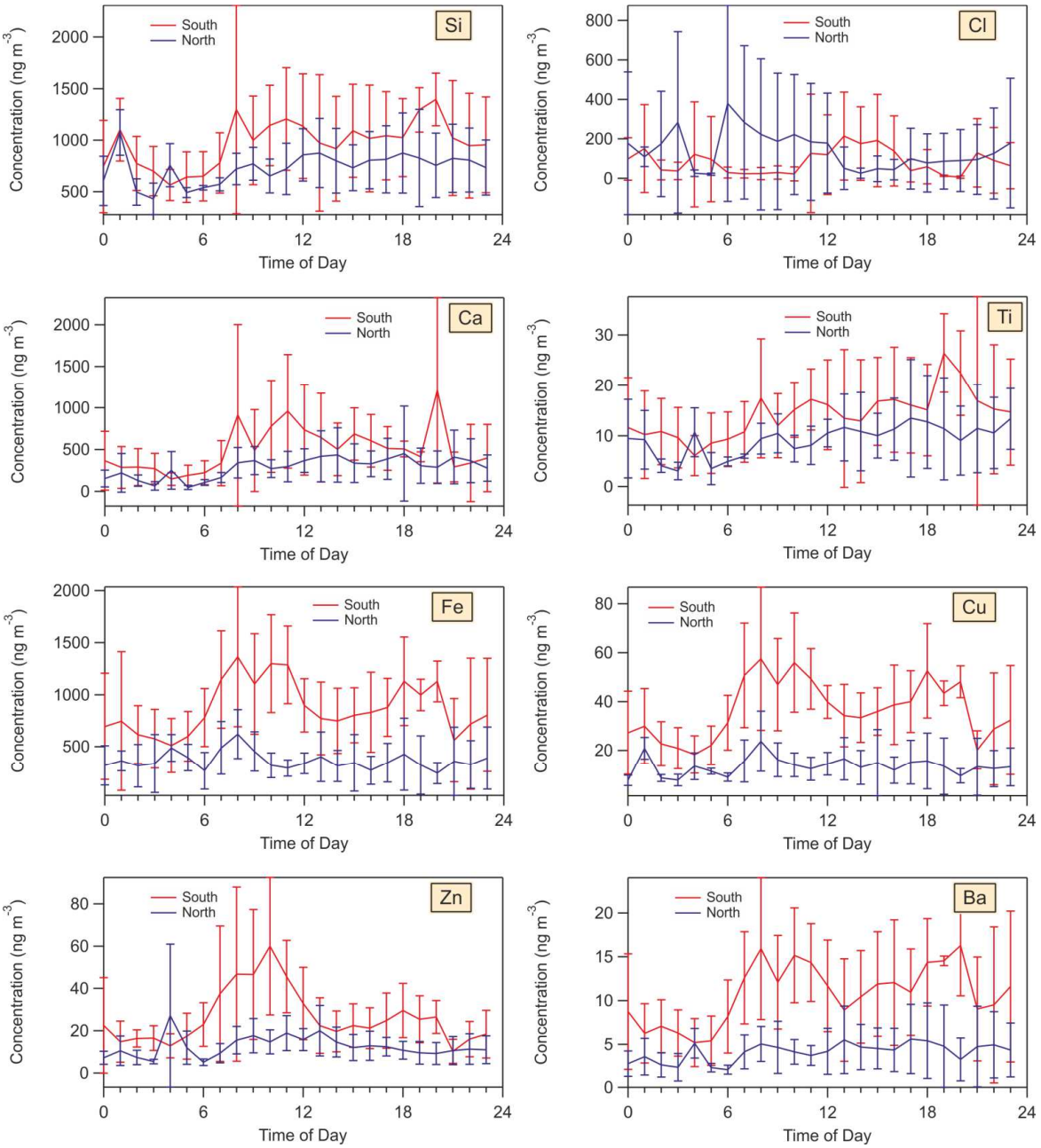

Figure S5: Diurnal variations of the Group A elements Si, Cl, Ca, Ti, Fe, Cu, Zn, and Ba. South means a wind from the freeway towards the station. See Fig. 8.

Reference

Tanner, T. M., Young, J. A., and Cooper, J. A.: Multielement analysis of St. Louis aerosols by nondestructive techniques, Chemosphere, 3, 211-220, 1974.